Proposal for the ^{252}Cf source upgrade to the ATLAS facility

Physics Division, Argonne National Laboratory

Contact persons: Guy Savard, Richard Pardo

February 22, 2005

Abstract

Beams of accelerated exotic neutron-rich nuclei allow access to little known regions of the nuclear landscape that are important both structurally and for r-process nucleosynthesis. We propose to increase the radioactive beam capabilities of the ATLAS accelerator facility by the installation of a new source of ions to provide beams of short-lived neutron-rich isotopes. These isotopes will be obtained from a 1 Ci ^{252}Cf fission source located in a large gas catcher from which the radioactive ions will be extracted and transferred to an ECR ion source for charge breeding before acceleration in the ATLAS superconducting linac. The technique is fast, universal and highly efficient. It will provide accelerated neutron-rich beam intensities of up to $7 \cdot 10^5$ ions per second on target at energies that are difficult to access at other facilities. This upgrade will enhance the reach of ATLAS and offer world-unique capabilities to study neutron-rich nuclei. It will also help advance technologies critical for the RIA facility.

I. Summary

Low-energy nuclear physics is at a very exciting time. The field, through both experimental and theoretical advances, has developed an "ab initio" understanding of the lightest nuclei starting from the nucleon-nucleon and 3-body forces, and an effective understanding of the heavier nuclei easily accessible in the laboratory. There is also a clear path to join these approaches from which an unified theory of most nuclei will emerge. Facilities, such as ATLAS, will play an important role in this quest. There are also indications from the region of very neutron-rich nuclei that the effective interactions are modified. This is the new frontier for low energy nuclear physics, where new phenomena are expected and a deeper understanding of so far untractable degrees of freedom will emerge.

The research interests in the field are moving in this direction but will have to await RIA to reach the most remote regions. In the meantime, progress can be made with more limited facilities that will guide the way and help develop the techniques and expertise necessary to explore neutron-rich nuclei. Some neutron-rich radioactive beam capabilities exist at present facilities, but some of the requirements for a number of important studies are not met. We have taken a critical look at these requirements for basic classes of experiments and developed an upgrade plan for ATLAS that will address these issues. The plan is based on ion source and ion extraction techniques developed for RIA to be used in conjunction with a strong californium fission source. When combined with the high efficiency post-acceleration that ATLAS can provide, this will produce

beams of sufficient variety and intensity to address the core scientific questions. The upgrade plan is described in the following pages where it is demonstrated that the new technologies allow the important requirements to be met at a modest cost. The project is highly complementary to other efforts worldwide since the fission fragment distribution from californium is different from that from uranium and production is focused on nuclei that cannot be extracted by any of the present ISOL facilities, including HRIBF and ISAC, nor future ones, such as MAFF and SPIRAL2. It is a timely opportunity that has great physics and technical synergy with RIA and will help develop a map to guide the community in its future quests.

II. Table of Contents

III. Scientific Justification

Our understanding of nuclear structure has evolved in stages, frequently driven by technological advances. Light ion induced reactions allowed the investigation of stable nuclei and the resultant explosion of new information stimulated the development of the shell model and collective models. Accelerated heavy ions allowed us to move away from the valley of stability and progress to very high spin. The curvature of the valley of stability allowed roughly a thousand new proton-rich isotopes to be studied. Again, this wealth of information stimulated theory and a new generation of mean field models and techniques for cranking the mean field to understand the effects of fast rotation. Now we approach a third phase. In this case theory and experiment are advancing together. In theory, the development of ab initio methods has moved our understanding of structure of light nuclei onto an entirely new quantitative plane with strong predictive power and high precision. In experiment, the challenge of very neutron-rich nuclei with completely new topologies such as neutron halos and skins has been glimpsed at, and accelerated radioactive beams are seen as the practical way to make progress.

The neutron rich "terra incognita" in which thousands of isotopes lie, and about which we know little, has already been shown to be full of surprises. At the dripline, where binding is the weakest, extensive "halos" of low density neutron matter have been found in light nuclei. In several cases the dripline was found to extend further than expected. Nearer stability, strong modification to the normal sequence of single-particle states has been observed, leading to new shell gaps and new shapes. There are also strong indications,

from the isotope production in the r-process for example, that the pronounced shell structure we are familiar with close to stability is altered in weakly bound neutron-rich systems. Standard nuclear reactions tend to populate the proton-rich side of the nuclear chart and, as a result, the neutron-rich region of the nuclear chart has remained mostly uncharted. Exploring the far reaches of this region is a key component of the RIA scientific program. And while the full capabilities of RIA will be required to thoroughly explore this region, interesting forays in this new territory would yield extremely useful information provided intense neutron-rich isotope beams at Coulomb barrier energies were available. The californium source upgrade to ATLAS proposed here will provide an array of neutron-rich radioactive beams, including isotopes that have not been amenable to ISOL techniques before, at sufficient energy and intensity to provide a first glimpse at the key nuclear properties and help delineate some of the parameters required of the RIA research programs. The section below highlights the physics goals and proposed approaches for the initial investigations the californium source upgrade project will allow. The first four physics topics presented below can be investigated with the existing array of experimental equipment present at ATLAS, the fifth physics topic gives an example of new programs that could be initiated with modest investment (programs that could easily be initiated by users), and the last topic points out the unique capabilities that the ATLAS californium upgrade presents to study stockpile stewardship issues.

A. Single-particle structure in the vicinity of magic nuclei

An important foundation of the description of nuclei is the characterization of the single-particle structure of stable nuclei near closed shells. These studies have provided critical information from stable nuclei on the ordering of single-particle states. Additional information near closed shells also provides the effective interactions between the nucleons in nuclei, that are the foundations of most modern nuclear models. It is expected that for the very neutron-rich isotopes the interactions will be modified by the neutron excess and the weaker binding and more diffuse nature of the neutron distribution. These changes could best be quantified by measurements of the single-particle structure on nuclei in the vicinity of closed shells in the neutron rich regions beyond stability. For short-lived nuclei, such measurements have to be performed in inverse kinematics with radioactive beams of energy well matched to the momentum transfer in single-nucleon stripping or pickup reactions. A prototype for such reactions are the neutron-adding stripping (d,p) or (α,^{3}He) reactions with a ^{132}Sn beam on a deuterium target.

It is important in such studies to be able to determine the angular momentum transferred in the reaction and this requires that both the entrance and exit channels be well above the Coulomb barrier. Expected angular distributions for a neutron pickup with the Q value equal to that to the ground state of ^{133}Sn with the above mentioned ^{132}Sn(d,p) reaction are shown for different energies in Figure 1. It is seen there that the cross-sections increase rapidly above the Coulomb barrier and that the angular distributions become much more

distinctive. For the (d,p) reaction on Sn, the optimum energy is around 7.5 MeV/u. Pioneering work is being carried out at Holifield on this reaction at the sub-Coulomb energies 4.7 MeV/u that are an extremely useful first step. However to be able to assign high-l states (such as the $i_{13/2}$) higher energies are essential, and the sensitivity of the cross sections at sub-Coulomb energies to the exact radius also favors higher energies for more quantitative measurements of the spectroscopic factors, to establish whether the states are indeed single-particle in character. The high-l states will still be relatively weak in the (d,p) reaction, however in (α,^{3}He) above ~ 10 MeV/u they stand out with unique strength (see Figure 2). Yields will be on the order of tens of counts/day per single-particle state for beams on target of 10^4/s for the (d,p) reaction, and a few a day for high-l single-particle states in (α,^{3}He).

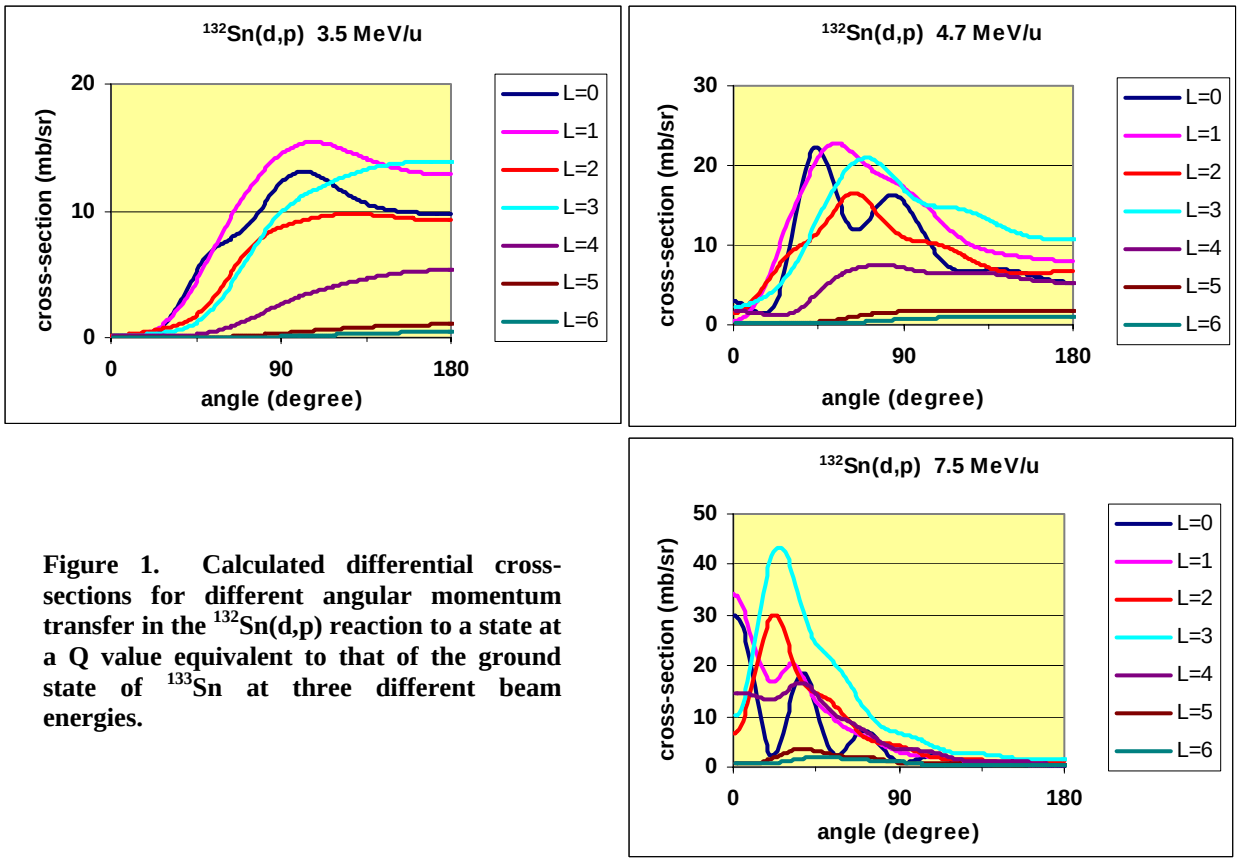

Figure 1. Calculated differential cross-sections for different angular momentum transfer in the ^{132}Sn(d,p) reaction to a state at a Q value equivalent to that of the ground state of ^{133}Sn at three different beam energies.

While ^{132}Sn is mentioned as an example, the measurements over the whole region of neutron rich nuclei would be of interest, including close to the N=50 line above ^{78}Ni. Obtaining information on the angular distributions requires radioactive beams of about 10^4 particles per second with now standard segmented silicon detector arrays. A facility that can not only provide the required energy, but also has a fast universal extraction technique that can allow a whole region of neutron-rich beams to be studied, is needed for such studies so that, for example, the yield of neighboring isotopes like ^{133}Sn ($t_{1/2}$ = 1.45s) is not orders of magnitude below that of the central ^{132}Sn ($t_{1/2}$ = 39.7s) isotope. Novel instruments such as the solenoid spectrometer [1] being proposed at Argonne could further reduce the required beam intensity, maybe by a factor of 2 or 3.

It is important to emphasize, that such studies will be a major area of investigation with RIA whose capabilities will greatly exceed those of the proposed upgrade. However the ATLAS Cf upgrade will open up considerable ground, complement the pioneering work at Holifield, and begin an exploration into the foothills of the regime that will be addressed by RIA, helping to refine experimental techniques in the process.

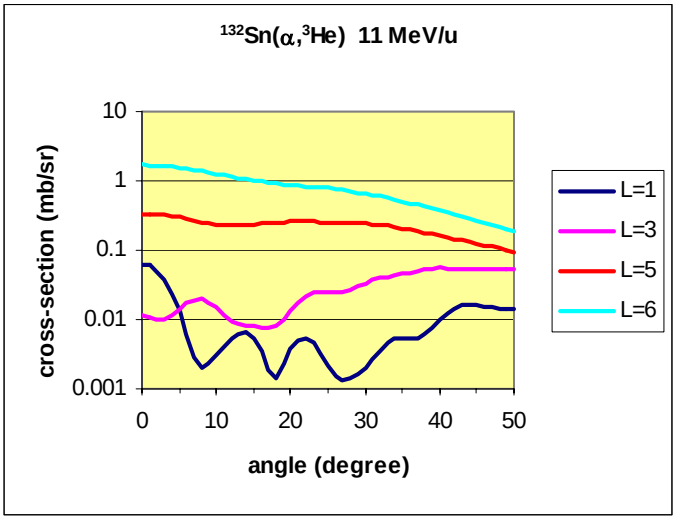

Figure 2. Calculated differential cross-sections for different angular momentum transfer in the ^{132}Sn(α,^{3}He) reaction to a state at a Q value equivalent to that of the ground state of ^{133}Sn. This reaction is matched most effectively to higher angular momentum transfer.

The (d,p) reaction can also play an important role in obtaining information for the (n,γ) rates on neutron-rich nuclei which must be determined to verify the validity of the steady state approximations used in many r-process models. Characterizing the states near the neutron threshold, and the bound states to which capture would occur can be carried out for a number of cases.

B. Pairing interaction in neutron rich nuclei

The pairing interaction plays an important role in nuclear structure. Measurements using nucleon-pair adding or removing reactions such as (p,t), (t,p) and (^{3}He,n) on stable nuclei were important in determining its nature and strength. It is, however, possible that the pairing interaction determined in stable nuclei will be modified in neutron-rich systems by the lower nuclear density. The two-neutron pairing interaction in weakly bound neutron-rich nuclei could be determined by measuring the energies and strengths of excited 0+ states (paired neutron particles or holes) using (p,t) and (t,p) reactions on neutron rich nuclei. In simple BCS theory all the strength is in the ground state and other excited 0+ states should be weak; in practice they are on the order of 1 % of the ground state. Where pairing breaks down, excited 0+ states are populated with much larger (10-30% of the ground state) strengths.

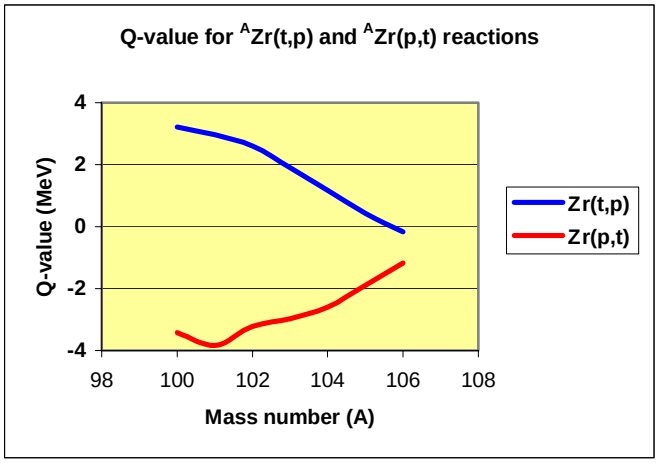

Figure 3. Q value for (t,p) and (p,t) reactions on neutron rich zirconium isotopes.

In the case of short-lived nuclei, these reactions are better performed in inverse kinematics at energies determined by the Coulomb barriers and the Q values. A typical example would be such reactions on neutron-rich zirconium isotopes for which the Q values are shown in **Figure 3**. It is observed that in this region of the nuclear chart the Q values for (p,t) reactions, reactions that bring us back towards stability, become more favorable as one moves away from stability. As a result, the (p,t) reactions on the most neutron rich isotopes and the (t,p) reactions on all nuclei can be performed with the energies of up to about 9 MeV/u that are available without stripping for A~100 nuclei with the current ATLAS accelerator. The (p,t) reactions on the closer to stability neutron-rich isotopes are best performed with the higher energies (see Table 1) that will be available after the current AIP funded ATLAS accelerator energy upgrade is completed. Using the proposed solenoid spectrometer the (p,t) reaction will yield on the order of 12 counts/day for 10^4 particle a second incident on a target – one would probably want at least 100 counts to set some limits on the fragmentation of pairing strength. These studies in more neutron-rich beams will be an important area of investigation with RIA and a start can be made with the proposed Cf upgrade to identify this behavior.

	Current ATLAS		UPGRADE I	
A	No Strip	Strip	No Strip	Strip
1	24.1	24.1	38.5	38.5
2	15.7	15.7	23.2	23.2
16	13.0	15.7	18.5	21.5
40	12.4	13.4	17.5	19.9
58	9.9	11.8	13.5	17.9
78	9.5	11.2	12.8	16.7
132	8.0	9.3	10.4	13.4
197	6.6	7.9	8.4	10.9
238	6.4	7.4	7.9	10.0

Table 1. Energies in MeV/u available at ATLAS without and with stripping for ions of various mass with the existing configuration and after the ongoing AIP funded accelerator upgrade.

C. Gamma ray studies of neutron rich nuclei

Accelerated fission fragment beams near the Coulomb barrier offer interesting opportunities for gamma-ray studies with Gammasphere. The mass and charge distribution of the fission fragments from californium cover highly deformed nuclei and the shape transitions in the A~100 and A~130 regions that provide an excellent complement to studies of spherical nuclei near ^{132}Sn performed at Oak Ridge following proton-induced fission of uranium.

The phase transition between spherical and deformed nuclear ground states has received a lot of attention recently as the nuclei at the transition points have been shown to have unique signatures. The californium fragments cover several important shape transitions. Some are first order like the abrupt shape change in the zirconium isotopes, while others are much more gradual second order changes, for instance in the barium and cerium

isotopes. The regions where the fragments are copiously produced should allow "vertical" isotonic phase changes to be delineated near N=64 and N=90 for the first time. The experimental test of these transitions lies in following the collectivity of yrast and non-yrast structures and observing how they cross and mix. Coulomb excitation of the accelerated fission fragments at energies near the barrier is a precise and discriminating tool for this research. The high degree of symmetry of Gammasphere and its good efficiency are perfectly matched to these experiments. The use of very inverse kinematics, using a beryllium or carbon target followed by residue identification, has been shown at Oak Ridge [2] to allow spectroscopy of very weakly produced exotic isotopes in a "cocktail" of isobarically mixed beams.

The nature of single-particle states in very neutron-rich nuclei is of major interest, as it allows us to seek evidence for isospin dependent modification of residual interactions. One of the more precise tests of the composition of nuclear wave functions is through measuring nuclear magnetic moments. A precise technique that is suitable for fission fragment beams uses the transient fields encountered by fast moving highly stripped ions. Coulomb excitation of the fragment beams allows interesting states to be populated and aligned in a known fashion, then the subsequent precession caused by the interaction of the nuclear moment and the field can be followed by measuring the decays. Again, the high degree of geometric symmetry makes Gammasphere an ideal tool for this research.

In the light fragment mass peak, around ^{104}Zr, lie nuclei with some of the largest ground state deformations known, $\beta_2 \sim 0.4$. Accelerated beams of short-lived isotopes of

zirconium (and most neighboring elements in fact) are not available at existing facilities. Prompt spectroscopy of gamma rays emitted following fission have provided some information on low-lying states in these nuclei, but Coulomb excitation of mass separated and accelerated beams would allow the microscopic structure of these collective modes to be established and their stiffness against beta and gamma vibration, and rotation, to be investigated. These nuclei have been predicted to have even more highly deformed structures at high spin. Whether these states can be populated by inelastic excitation depends on the degree to which the configurations mix. If the shape evolution is adiabatic then population may be possible, but if the configurations are well separated, as is found in most superdeformed nuclei, they will be more difficult to probe.

^{104}Zr provides a good case for a more quantitative insight of gamma ray experiments possible with the proposed upgrade. Its ground state deformation and low-lying levels are already known from recent prompt gamma spectroscopy of emissions from a fission source. Extrapolating these properties, and assuming rigid rotor behavior to the very highest spins, allows the calculation of expected yields in a conventional thin target Coulomb excitation study, for example using CHICO (the Rochester chamber for studying inelastic scattering) and Gammasphere. For example, with a beam of 2 x 10^4 particles per second on a lead target at a safe energy for electromagnetic excitation, the first excited state is populated with a cross-section approaching 5 barns and 100 hours of data collection would yield ~10,000 photopeak decays, about 2/3 of which would have at least 1 coincident gamma ray full energy photopeak from multiple excitation. Even a few decays from the (unknown) J=20 state should be detectable. For "pure" beams, stopping

in a thick target would enhance yields by a factor 2-5, and allow crosschecks of collectivity through fitting DSA line shapes. Increasing the beam energy into the "unsafe" region where both electromagnetic and nuclear processes occur would also enhance the yields at the cost of losing the predictability and cleanliness of Coulomb excitation. In addition, the higher energies would allow few-nucleon transfer studies populating neighboring nuclides. In most cases the interesting spectroscopy would involve identifying new states in coincidence with the known low-lying levels so that a considerable level of contamination from a "cocktail" beam could be tolerated.

Another collective mode in this region is that of octupole collectivity. Neutron-rich barium and cerium nuclei are known to exhibit features consistent with significant octupole collectivity, probably vibrational, but discriminating tests can only come from measuring dipole and octupole matrix elements. These measurements have not been possible up to now, but are straightforward in Coulomb excitation studies with the proposed beams.

The issue of using fission fragment beams to induce fusion reactions is worth consideration as a tool for studying even more neutron-rich nuclei. In general, reactions on heavy targets do not look promising, as the fused systems tend to lie close to the valley of stability, due to its curvature, and neutron evaporation is calculated to be very probable. However, this method may be important in some cases to populate high spin isomers that cannot be reached by other means. A further possibility is the investigation

of fusion with neutron rich targets, like ^{14}C, and observing charged particle evaporation from the compound nucleus to tag the production of nuclei far from stability.

D. Nuclear properties and decay studies along the r-process path

The r-process is responsible for the formation of roughly half of the nuclei above iron. The high neutron flux and high temperatures that occur in explosive events such as type II supernovae explosions or possibly neutron star mergers convert seed material into heavier elements via a series of neutron captures and beta decays. Neutrons are captured on the seed nuclei via (n,γ) reactions leading to more and more neutron-rich nuclei. Simultaneously, the high temperature generates a high flux of thermal gamma rays that can destroy these neutron-rich nuclei via (γ,n) reactions. The competition between these reactions yields an equilibrium distribution of neutron-rich isotopes of a given element determined by the temperature and the neutron separation energies. Beta decay provides a path to the next heavier element where the (n,γ) and (γ,n) reactions again yield an equilibrium distribution for neutron-rich isotopes of this next element. The neutron flux is large enough for the reactions to be much faster than the beta decay rates and so the process continues and leads to heavier and heavier elements via a path situated far on the neutron-rich side of the nuclide chart. It is estimated that the event lasts only one to tens of seconds after which the created neutron-rich isotopes decay back to stability to yield the observed isotopic distribution.

The path followed by the r-process is determined by the ground state properties of the neutron-rich isotopes involved. The location of the path, for a given temperature, is determined by the neutron separation energies and hence the masses (mass differences) of these isotopes. The timescale to create the heavier isotopes is determined by the beta decay lifetime of the neutron-rich isotopes along the path. And, finally, the remaining isotope distribution that is the key signature of the r-process is affected not only by the beta decay lifetimes along the path, but also by the beta-delayed neutron emission probability. The path followed by the r-process is, however, so far from the valley of beta stability that most of the isotopes of interest have not been accessible in the laboratory. Figure 4 shows the limit of known masses together with isotope production from a californium source and an outline of the r-process path. Only a small fraction of the isotopes along the path have had even their most basic property, i.e. their mass, measured. The situation is only slightly better for the lifetime and decay properties. Modeling of the r-process therefore depends on extrapolation of the properties of known isotopes to region where we have reasons to believe the physics is modified. This is highly unsatisfactory and a more detailed understanding of the r-process requires obtaining an improved knowledge of the ground state properties of very neutron-rich isotopes.

The mass of a short-lived isotope can be measured to an accuracy of 10 keV/c^2 or better with the Penning-trap based CPT mass spectrometer and an isotope production of a few ions per minute. All isotopes identified in Figure 4 could have their masses measured to this accuracy, including roughly 180 very neutron-rich isotopes in the close vicinity of

the r-process path whose masses have never been measured before. This would require roughly half a year of measurement time with the CPT spectrometer connected to the low-energy diagnostics station that will be used to tune these beams.

Lifetime can be determined with similar or even lower yields with the isotopes identified with an isobar separator or by other means after post-acceleration. All isotopes identified in Figure 4 could have their lifetime measured this way. New, more neutron-rich isotopes with much weaker yield might also be discovered using such techniques.

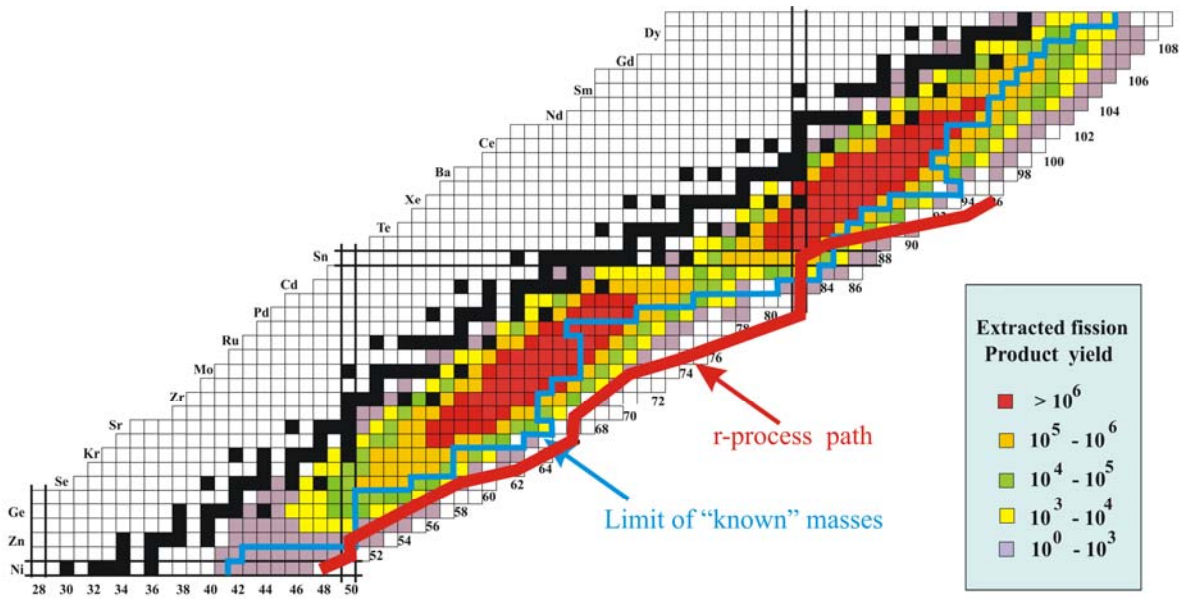

Figure 4. The r-process path together with the yield expected from an ion source system based on a 1 Ci californium fission source and the limit of known masses.

In addition, much of the decay data on neutron-rich nuclei that can be accessed through the Cf source are incomplete or completely missing which concerns both the nuclear structure and astrophysics interests. For nuclear structure, the determination of quantum

numbers, log ft, etc … and the elucidation of single -particle levels in odd-mass isotopes are important for the understanding of neutron-rich nuclei. For nuclear astrophysics, well understood level schemes are of importance, especially in predicting (n,γ) and (γ,n) cross sections along the r-process path. In addition, many of the odd-odd isotopes have two (or more) beta decaying states that may have significantly different lifetimes. There is a coupling of these states in hot stellar environments that in turn affect the decay rates along the r-process path. The structure coming from β-decay studies would be of importance to elucidate such effects. Finally, the beta-delayed neutron emission probability is required to calculate the final isotope distribution following the r-process and such measurements could be done here on a number of nuclei on the r-process path. In this case, as is the case for the lifetime and mass measurements mentioned above, the nuclei around the N=50 and N=82 closed shells are of particular importance for the r-process calculations and these measurements could be done in parallel to the mass measurements.

E. Laser spectroscopy of neutron-rich nuclei

Laser spectroscopy has been a key tool to investigate properties of the nuclear ground state and isomers of short-lived isotopes. Isotope shifts in atomic transitions reflect the change in charge radii between isotopes and are an excellent probe for nuclear shape transitions and halo phenomena. The hyperfine structure of atomic transitions reveals the nuclear spin, and the magnetic dipole and the spectroscopic quadrupole moment of the nucleus can be inferred from the energy splitting between hyperfine levels. These

experimental data are highly accurate, can be extracted independently of nuclear models and are very sensitive to both single-particle and collective properties. They therefore provide excellent tests for nuclear models.

Figure 5 shows the expected low-energy yield with the proposed ^{252}Cf fission source. The color-coded yield plot is laid over a chart of nuclides taken from [3] that highlights the regions for which laser spectroscopy has been performed on long isotopic chains or on nuclei far from stability. Collinear spectroscopy in combination with an ion cooler and buncher will be able to cover the region with yields of ~100 ion s^{-1} and above. Given the two fission yield maxima for neutron-rich isotopes in the intermediate mass range, there are two main opportunities for laser spectroscopy.

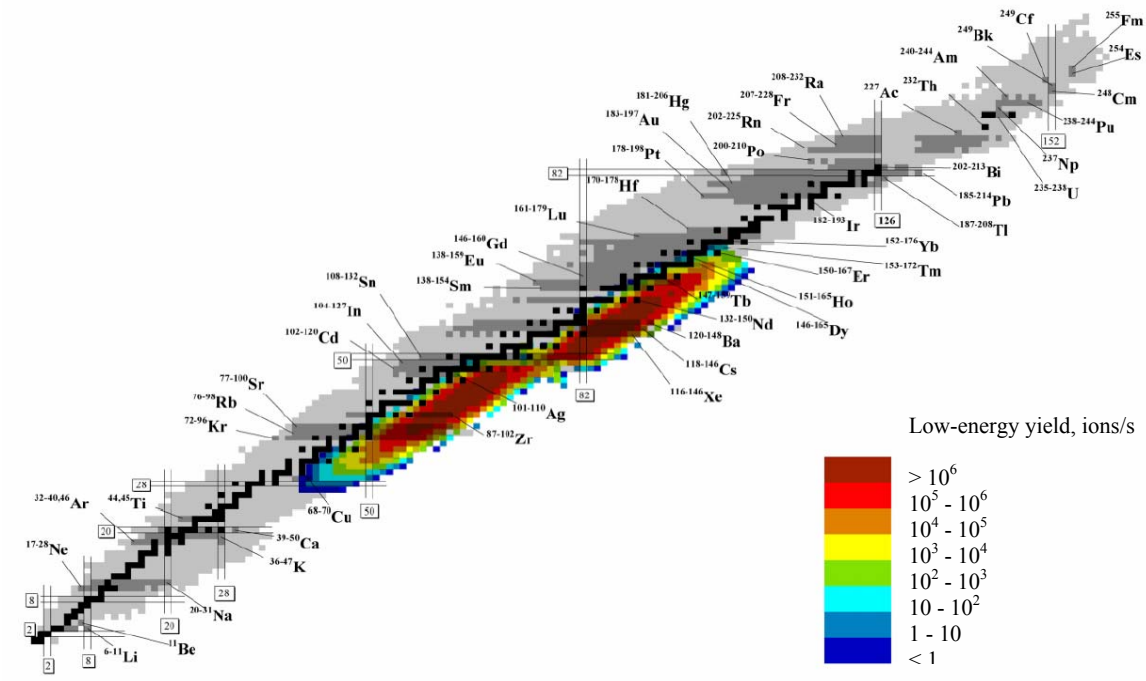

Figure 5. Chart of nuclides taken from [3] showing in dark gray the isotopes for which laser spectroscopy was performed on long isotopic chains or on nuclei far from stability. Black squares indicate stable nuclei, light gray are those nuclei known to exist as bound systems. The nuclear chart is overlaid by a color coded contour plot showing the projected ion yield at the low-energy beam line for a 1 Ci ^{252}Cf fission source.

The first is to continue the measurements of long isotope chains further to the neutron-rich side and to observe how charge radii and moments change by adding more and more neutrons. These investigations also have the potential of discovering previously unobserved isotopes and isomers. Isotope chains of interest are those of silver, cadmium, indium and tin. Of particular interest is the possibility to extend the existing data on indium isotopes to reach the N=82 shell closure at ^{131}In and to measure the nuclear properties beyond the double magic ^{132}Sn [4]. Additional areas of interest for continuing existing measurements and start the measurement of new isotope chains are the refractory elements from ytterbium to palladium [5] and very neutron-rich isotopes of the rare earth elements from lanthanum to holmium.

The second opportunity is to investigate the isotopes along the neutron-rich side of the largely unexplored N=50 shell closure from zinc to selenium and possibly bromine and to follow the N=82 shell closure further to antimony and tellurium.

F. Stockpile stewardship

Determining quantities of interest to the stockpile stewardship program will come naturally with the californium upgrade project. Determining the properties of neutron-rich fission fragments such as masses and, possibly, more accurate ground state lifetimes are among these. In addition, investigations of the neutron-adding (d,p) reactions on such nuclei hold important clues that can allow for more reliable estimates of neutron cross

sections on these isotopes. Other reactions may allow a check of the applicability of statistical properties to such nuclei that provide important checks. The proposed technique is particularly suitable for the explorations of the properties of neutron-rich isotopes of zirconium and yttrium that are of particular interest.

IV. Conceptual Overview

The neutron-rich region of the chart of nuclides is the next frontier in low energy nuclear physics and we have highlighted above some of the tools necessary to chart and understand this region. The task requires performing experiment with beams of short-lived neutron-rich isotopes in specific energy regimes. Interesting capabilities now exist for radioactive beams in this region at the Holifield facility and will soon exist at the ISAC and REX-ISOLDE facilities. Limitations in the species that can be extracted and the energy to which they can be accelerated however hamper the ability of these facilities to address a number of key physics questions. The ATLAS facility at Argonne has a unique potential in that it has the required capabilities and expertise to become, with a modest upgrade, a very cost effective facility to perform this research. In fact, with this upgrade, ATLAS will have radioactive beam capabilities that will be unmatched on a national and international scale. It will be an important tool to pave the way and prepare the field for the RIA era. It will also demonstrate in battle conditions many of the technologies that are critical to RIA.

The necessary steps to accomplish the task are (1) the production of the short-lived isotopes, (2) the rapid extraction and preparation of the selected isotopes, (3) their post-acceleration to the optimum energy for the particular experiment, and finally (4) the availability of the required instrumentation to carry out the experiments. New techniques developed at ATLAS for the CPT trapping program and for the RIA facility enable the stopping of fast recoil ions into a gas catcher and their rapid extraction as a low-energy beam of very good quality. This technique is applicable to essentially all species and is very efficient. We propose to use such a gas catcher to stop recoils from a 1Ci ^{252}Cf fission source and to extract them as a low-energy beam. This provides access to all species produced in the fission of californium. In particular, this puts within reach species which are difficult to extract by standard ISOL techniques and are not produced with low-energy fission of uranium. This approach therefore provides unique beams that will not be available elsewhere until facilities like RIA come along.

The californium source and gas catcher will be located, together with an RFQ gas cooler and an isotope separator, on a new high-voltage platform. This new platform will be located at ATLAS besides the ECR-1 high-voltage platform and have an independent high voltage control with output that can be compared and adjusted versus the ECR-1 high voltage. The extracted isotopes are transported and cooled in two sections of RFQ gas coolers yielding beams with very low transverse emittance and energy spread. The beams are then accelerated to 50 keV and sent to a high-resolution mass separator where a specific isotope is selected. The very good beam properties extracted from the gas cooler allows one to obtain a mass resolution of 20000 with a one-stage separator that is a

scaled down version of the isobar separator that has been designed for low-energy beam purification at RIA. Two beamlines will be attached to the isobar separator; a low-energy beamline for tuning/diagnostics and low-energy experiments, and a beamline leading to the existing ECR-1 high voltage platform. Most unwanted activity will be stopped in the mass separator and remain on the first high-voltage platform. This platform is expected to be the only location where sizable accumulation of radioactive isotopes will occur.

Post-acceleration of the low energy beams extracted from the first platform must be done efficiently. In the context of RIA, a large effort has been devoted at Argonne to develop high efficiency approaches to perform the post-acceleration of low charge-state ions. It was determined that the most efficient approaches require an ATLAS-like high-acceptance superconducting linac. In fact, ATLAS is proposed as a component of the post accelerator if the RIA facility is sited at Argonne. The main approach for post-acceleration at RIA will use low-velocity RFQs and non-equilibrium charge state stripping to then inject into an extended low-energy section similar to the existing ATLAS PII linac before completing the acceleration in the booster and ATLAS sections. This approach is the most efficient at all energies and, in particular, shows the highest gain over other approaches for astrophysics type energies below 1-1.5 MeV/u.

A second [6,7,8] approach, inferior at very low energy, but almost as efficient at Coulomb barrier energy, will also be used at RIA. A charge-state breeder will be used to increase the charge state of the singly charged radioactive ions so that they can be accelerated directly in ATLAS. This will provide an independent acceleration route to

the experimental area for physics at the Coulomb barrier that can be used during long experiments in the astrophysics area. It will greatly enhance the multi-user capabilities of RIA. We propose to use this same approach in this upgrade. For the mass range covered by fission fragments and at the Coulomb barrier energies which are of interest for the proposed physics program it yields almost the same efficiency as the full RIA post-accelerator but at a much lower cost.

The ECR-1 ion source will be modified to be used as a charge-state breeder (it will remain usable as an ECR source for normal ATLAS operations). The mass selected singly (or doubly) charged ions will be injected into the ECR-1, their charge state increased by the plasma, and they will then be extracted and sent to ATLAS in a fashion identical to normal stable beams.

Only minor modifications to ATLAS will be implemented for this upgrade. The energy range that will be accessible after the current AIP funded ATLAS energy upgrade is completed will be sufficient to address the physics questions put forth above. Transmission of the ATLAS accelerator is very high, limited in theory only by the bunching efficiency that should be up to 85% with the multi-harmonic buncher currently in use. In practice, there are a few “apertures” in the beamline that are there for historical reasons and that limit the tuning range available making the highest transmission efficiency difficult to obtain. They will be removed. Diagnostics will also be improved in the injection into ATLAS to obtain better tunes for standard beams and extend their

usefulness to lower intensity beams. Both of these actions will be taken to provide the highest post-acceleration efficiency possible.

Finally, ATLAS already possesses first class instrumentation for most of the studies being proposed with Gammasphere, the FMA, the CPT mass spectrometer, and the Ludwig detector array and Enge spectrographs. In addition, a proposal has been submitted for a solenoid spectrometer for reaction studies with radioactive beams that would further enhance the existing capabilities.

V. Technical Description

The various components of the upgrade presented above will be described individually in more details below.

A. Source of radioactive isotopes

Neutron-rich isotopes are generally obtained from proton, neutron or photon induced fission of uranium. Low-energy proton-induced fission of uranium is used effectively as a source of neutron-rich isotopes at the sole US facility with accelerated fission product beams, HRIBF at Oak Ridge. This approach has well defined production peaks and little production outside these regions. In addition, further limitations in the species extracted are present with the standard ISOL methods and the post-acceleration schemes used. The physics program proposed above requires access to isotopes not available with existing

facilities in the US or abroad. This requires both a different production technique and a more universal extraction approach. Different approaches to producing the neutron-rich isotopes have been investigated and it was concluded that fission sources are a promising alternative to beam induced fission.

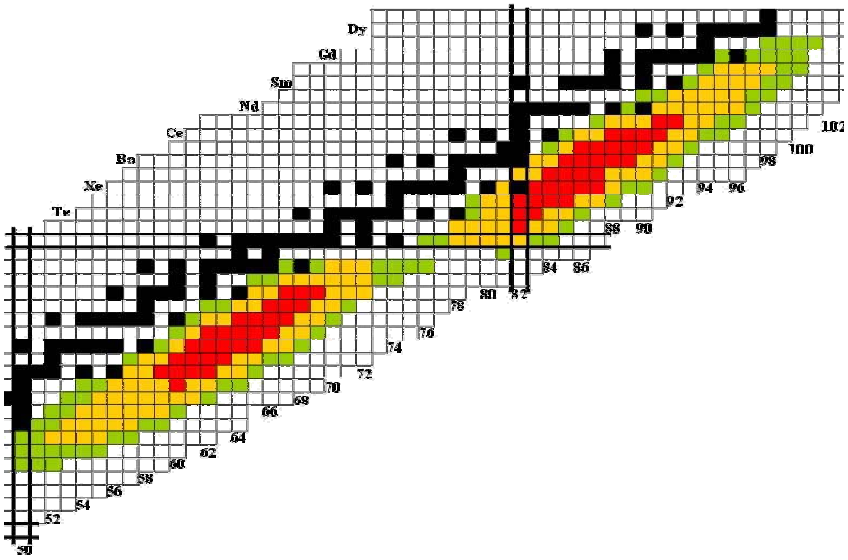

Figure 6. Distribution of the fission products from the spontaneous fission of ^{252}Cf. Both peaks are centered on heavier mass than the equivalent peaks in uranium fission.

Of the available fission sources, ^{252}Cf was selected as best suited to our application. The fission fragment distribution is peaked in regions of physics interest (see Figure 6) that are not populated well by uranium fission. With its 2.64 years halflife and a 3.1% fission branch, ^{252}Cf has a large specific activity so that attenuation of the fission fragments in the intrinsic source thickness is not an issue and the source does not have to be replenished too often. A working program at Oak Ridge produces ^{252}Cf sources on a commercial basis. They can produce sources of the required strength in various forms. The CPT program at Argonne uses californium sources from that supplier, electrodeposited on a thick tantalum backing. These are robust and well suited to our

application since the fission fragments have a 2π solid angle to escape the source and backing and be subsequently captured in the gas catcher.

The source will have a total activity of 1 Ci and be electrodeposited on a flat 0.1" thick tantalum backing located on a source holder (similar to that used in [13]). The deposition will have a diameter of 5 cm, yielding a density of 51 mCi per cm^2. Californium sources with 5 mCi per cm^2 density (0.6 mCi over a 0.4 cm diameter spot) are currently in use at the CPT spectrometer. No sign of flaking or any other form of activity loss has been observed under these low-density conditions. Stronger electrodeposited open ^{252}Cf sources were also prepared at Oak Ridge for the gas jet system [12] at Idaho National Engineering Laboratory with total activity of 0.25 Ci over a few cm^2. That source density exceeds our requirements and it was successfully operated there. The 1 Ci source will be inside the gas catcher and be covered by a 2 mg/cm^2 gold foil located one mm above the source for protection and confinement. It will enclose the source, except for a pumping hole to equilibrate pressure inside the trapped volume with the gas catcher pressure. The foil will be mounted on the source by remote handling in the chemistry hot cell after reception of the source at Argonne, using techniques similar to that used in [13]. An additional degrader will be supported above the gold foil to tailor the energy loss of the recoils to the geometry of the gas catcher as explained below.

B. Gas catcher and degrader

The critical step in the production of radioactive beams is the efficient transformation of the activity into a low energy beam that can be further accelerated. As mentioned above, this step must be as universal as possible to access the difficult elements that are of physics interest. Efficiency is also critical since it determines not only the final yield, but also the size of the radioactive inventory that has to be handled and shielded. The gas catcher technique, an approach combining both universality and high efficiency, has been developed at Argonne first for injection into the CPT mass spectrometer and then for the RIA facility [9]. It is ideally suited to this task.

The gas catcher thermalizes incoming radioactive ions as singly or doubly charged ions that are then extracted as a cold beam by a combination of DC fields, RF fields, and gas flow. The californium source will be located at the entrance of the gas catcher; the fission fragments will be slowed down in a degrader foil and then stopped in high purity helium before being extracted. Gas catchers have been in operation at ATLAS for about 5 years and the basic operational principles are now well understood. The initial step in designing a gas catcher for this specific application is to determine the volume of high purity helium gas that is needed to thermalize fission fragments of a given range. Studies were performed with the Monte Carlo version of the code SRIM to determine the effective range distribution obtained with various degrader configurations in front of a californium source.

From such studies, it was determined that a gas catcher with a gas pressure of 150-200 mbar, an inside diameter of 25-30 cm and a length of 60 cm would be best suited to stopping both light and heavy fission fragments. For such a volume and for a specific degrader configuration, most of the fission fragments emitted into the open 2π solid angle will be stopped in the gas. The radioactive ions are thermalized as singly or doubly charged ions in the high purity helium gas and must then be extracted from the gas volume before they decay or are lost to charge exchange processes with impurities in the gas or to collisions with the chamber walls. To avoid any appreciable losses, the extraction must be performed on a time scale of 20 ms or less, much faster than can be achieved by gas flow alone. This is obtained with the gas catcher concept developed and successfully used at Argonne. It utilizes a combination of DC and RF fields superimposed on the gas flow to effectively and quickly extract the isotopes stopped in high-purity helium gas. The combination of the three forces provides: fast transport through the main part of the device (DC field), focusing toward the extraction nozzle (RF field), and rapid extraction through the nozzle (gas flow). This scheme allows the use of a much larger stopping gas volume than would gas flow alone, as well as the handling of much higher intensities than a DC field-based system.

The ionization in the gas catcher needs to be considered. The gas catcher scheme was first demonstrated at ATLAS and is now a central component of the very successful physics program at the CPT mass spectrometer. This scheme overcomes the limitations of some of the earlier gas stoppers. At present, it has been used with ionization of over

10^{11} helium-ion-electron pairs per second in a cell with a volume of 0.8 l. With a 1Ci source, including the contributions from both the alpha particles and fission recoils, one expects roughly 4.5 X 10^{14} helium-ion-electron pair per second in a volume of ~45 l. This corresponds to about a factor of 60 beyond the present experience. However, this is still roughly 10 times lower than what is required for the RIA application. A test of the RIA gas catcher at high-intensity is in preparation at ATLAS as part of the RIA R&D and calculations indicate that it will be sufficient to handle the space-charge repulsion created by such a charge cloud. This intensity is too low to create any "plasma" effects. The main issue here becomes one of helium gas purity since the helium ions can be handled fairly easily as long as they do not transfer charge to contaminants; measures to maintain the gas purity required are discussed below. It should also be noted that helium ions that are created do not leave the gas catcher; only the heavy ions (and charged heavy impurities) are extracted so that the current in the subsequent devices is much lower than in the gas catcher. The requirements for the present application can be fulfilled by a shortened version of the RIA gas catcher prototype.

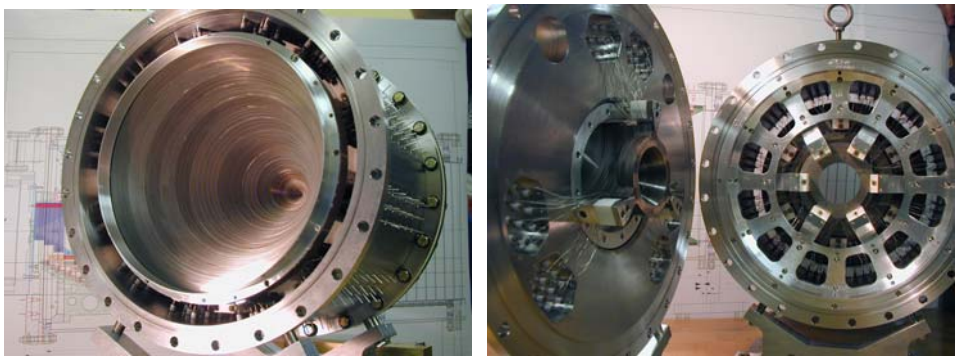

Figure 7. View of the extraction region of the RIA gas cell prototype. This section consists of 279 plates operating with RF voltage applied between the odd and even plates to focus the ions to the extraction aperture.

The full-scale RIA gas catcher prototype is a complex yet reliable device with more than 7400 components. Figure 7 shows the extraction section of the RF cone, the most complex section of the device. Strong RF fields on the 279 plates forming the cone create an RF wall that does not allow the radioactive ions to come closer than a few mm to the cone while they are dragged forward by the DC field until the gas flow takes them out via the final nozzle at the cone apex. The extraction cone is attached to the gas catcher main body composed of modular cylindrical sections. These sections provide most of the stopping volume and a strong DC field that moves the ions forward towards the RF cone and extraction nozzle. The RIA prototype gas catcher (see Figure 8) used 7 cylindrical sections connected to the RF cone chamber, the gas catcher for the californium upgrade will use a similar RF cone connected to 3 cylindrical sections, the first section hosting the fission source and degrader.

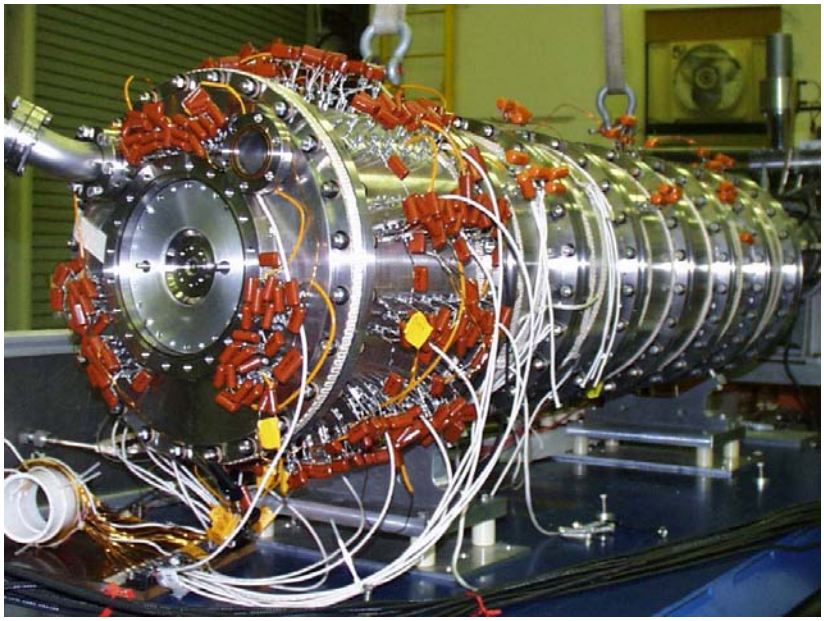

Figure 8. Assembled RIA gas catcher prototype with tuned circuit to provide RF and DC potentials to the body and cone electrodes. The extraction nozzle and chamber hosting the extraction cone can be seen on the left side of the picture.

The gas purity requirements in the gas catcher are extremely high. It operates with a continuous helium gas flow of 10 SLM. This is equivalent to a continuous pumping speed of roughly 1 liter per second. Maintaining the required ppb level purity in the helium therefore sets an upper limit of 10^{-7} Torr-liter/second for the total outgassing rate inside the gas catcher. This can only be achieved with UHV materials and techniques applied to the gas catcher fabrication. This was obtained in the RIA prototype gas catcher by using only metal and ceramics in the construction and using indium seals to join the different sections. A similar construction approach will be used here, except for minor modifications to make the system more modular and capable of sustaining baking at higher temperatures. This will be done by replacing the large insulator rings used in the RIA prototype by an insulating enamel coating and the indium seals by Helicoflex all-metal seals. These all-metal seals on enamel surfaces are radiation resistant, easy to replace and reliable. The gas flow of 10 SLM is small enough to be accommodated by a pumping system that can fit on a high voltage platform. The helium gas is coming from cylinders that are stored off the high voltage platform. The gas is brought up to the high voltage platform at high pressure in an electrically insulated line. It is then purified in a cold trap and transported in an all-metal distribution system first to a Monotorr solid state purifier (SAES Getters) for further purification before finally being fed to the gas catcher.

The required radioactive ion extraction time is attained with a total DC voltage of roughly 1000 volts along the gas catcher. A total RF power of about 1 kW is needed to provide the 1 MHz RF field required on the RF cone with its roughly 100 nF capacitance. This is obtained with an air-core inductance forming a tuned circuit with the cone plates and the

voltage distribution system, with the circuit fed by a 150 watts RF amplifier. The gas catcher system is installed in a high-voltage cage enclosed in radiation shielding.

C. Transport cask

The 1 Ci ^{252}Cf source used to produce the radioactive ions is a major source of radioactivity. The main activity is high-energy alpha particles which can be shielded easily. The fission branch itself is, however, accompanied by the emission of neutrons which are a much more serious concern. In addition, the fission fragments emit betas and gammas which also require shielding. The unshielded source generates fields of about 44 rems/hr at 30 cm and can therefore be handled only remotely in hot cells and transported under heavy shielding. The source, deposited on a 5 cm diameter tantalum disk mounted on a source holder, will be brought to Argonne's existing hot cell facility located in the Chemistry Division building. Some refurbishing of the hot cell manipulators is required for this task and the resulting cost is included in this proposal. The source size is small enough for a standard commercially available and certified lead pig to be used for storage during transport from Oak Ridge to Argonne. There it will be remotely mounted on a support plug that fits in the back of the gas catcher (this is similar to the technique [13] used for the gas jet experiments at INEL with similar strength sources) and the thin gold foil mounted on it. The plug is installed in a large movable cask with about 60 cm borated polyethylene and lead shielding surrounding the source and plug (see Figure 9). Transport between the hot cells and the gas catcher is performed in the shielded cask by the Special Materials Group. The radiation limits they can handle are 200 mrem/hr on contact and 10 mrem/hr at 2 meters so that in principle a much smaller cask for the

transportation and more local shielding at the gas catcher could be used. At this point we are opting for the more conservative solution. The cask is moved to the high voltage platform at ATLAS and installed on rails to guide it to the gas catcher and its permanent shielding. The procedure to install the source inside the gas catcher is shown in Figure 9. The cask is pushed up to the permanent gas catcher shielding, the cask is opened and the source and plug moved forward and attached to the gas catcher, the pusher is pulled back into the cask and the cask closed. The cask remains in location and becomes part of the shielding for the gas catcher. The procedure is reversed to remove the source and plug from the gas catcher.

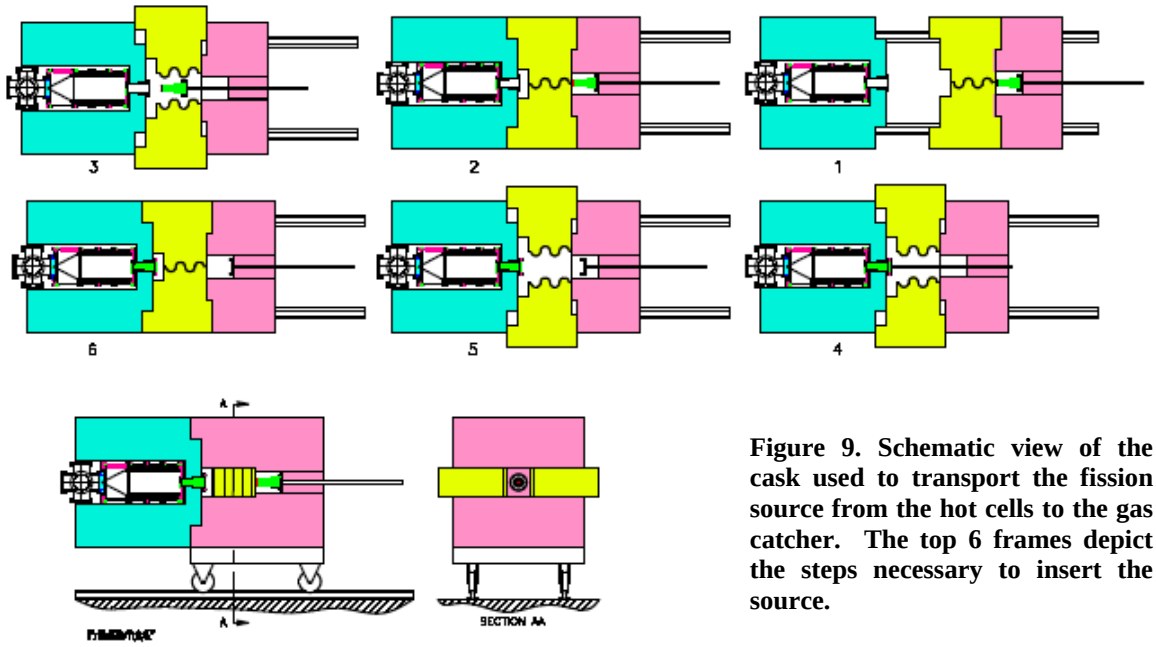

Figure 9. Schematic view of the cask used to transport the fission source from the hot cells to the gas catcher. The top 6 frames depict the steps necessary to insert the source.

D. RFQ gas cooler

The radioactive ions extracted from the gas catcher are extracted in the presence of a large gas flow. The gas pressure at the nozzle is high enough to disturb the acceleration

of the ions. The radioactive ions must therefore be transported at low energy to a lower pressure region before acceleration. This is done via open RFQ structures that guide the ions while letting the gas escape and be pumped way. The ions extracted from the gas catcher are therefore fed into two sections of RFQ cooler (see Figure 10) separated by a differential pumping aperture. Both sections are segmented longitudinally to add DC longitudinal gradients to the transverse RF focusing and use a large structure with rod separation of 15 mm to ensure that all ions extracted from the gas catcher are initially captured within the confining potential. Similar structures are used in the CPT gas cooler and the full scale RIA gas catcher prototype and in both cases no losses are observed in the process. The first RFQ section is pumped by a large blower while the second section is pumped by a turbodrag pump. After the second RFQ section, the pressure is low enough for electrostatic acceleration to 50 kV and transport to the beam preparation section. The ions are cooled by gas collisions in the RFQ structures so that the extracted beam properties are excellent with an energy spread below 1 eV and transverse emittance of roughly 3π mm mrad [10] at 50 keV. These structures are operated in a continuous mode and the total beam current extracted from them is small enough (of the order of a nA) to not affect the emittance.

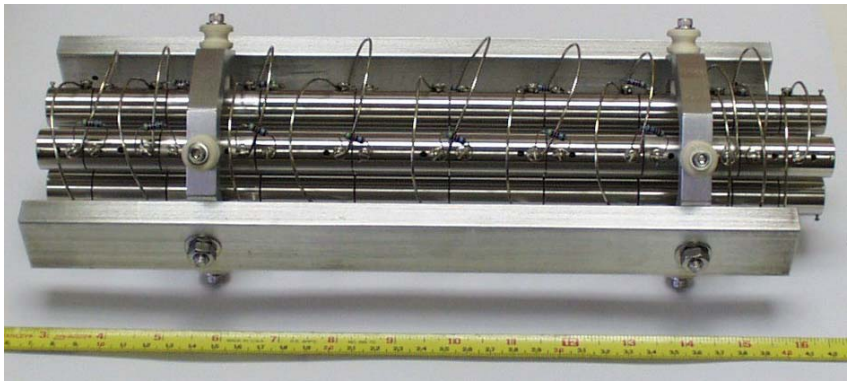

Figure 10. Section of RFQ cooler used to remove the ions from the high pressure region and further cool the radioactive ions.

E. Isobar separator

One of the great advantages of the approach being proposed here is the universality of the extraction technique that makes it possible to obtain beams of all species produced in the fission process. That advantage is maintained in the post-acceleration where the superconducting linac, with its large acceptance, accelerates efficiently all species. Some mass selection (actually magnetic rigidity selection) is present in the post-acceleration but for practical purposes it is limited to about 1 in 400 resolution, enough to remove neighboring masses but not isobars.

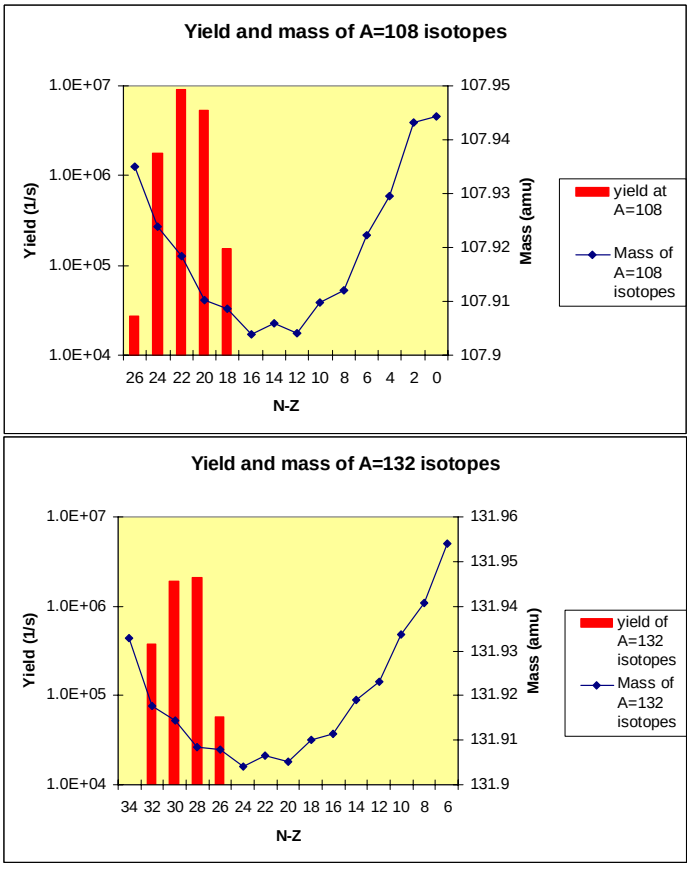

Figure 11. Plot of the masses and calculated low-energy yields for A=108 (top) and A=132 (bottom) isobars. The mass differences close to stability are 1 part in 20000-40000, while further away from stability mass differences in excess of 1 part in 10000 are encountered. However, the rapid decrease in intensity far from stability makes the suppression of isobars required more important.

Most experiments can tolerate some form of contamination or steps can be taken to separately identify the beam species. However, certain experiments will be adversely affected by the presence of contamination in the beam and it is therefore important to add some higher resolving selection in the system. We propose to perform this task with an isobar separator located on the gas catcher high voltage platform. This will not only improve the purity of the beams sent to experiments, but will also ensure that the bulk of the radioactivity extracted from the gas catcher system remains on the gas catcher high voltage platform. This confinement of activity should allow for the maintenance of components not located on this first platform to be essentially unaffected by this upgrade since no sizable radioactive inventory buildup is expected outside of this platform. It is also important to provide a beam as pure as possible to the charge state breeder to minimize the high charge state degeneracies which also affect beam purity.

The initial step in the selection of the isobar separation scheme is the determination of the required performance and of the expected beam properties. The required performance is set by the mass difference along isobaric lines and the relative abundance of the various isobars. This information is plotted for two representative cases in Figure 11. The combined effect of differences in mass and yield along an isobaric line can be seen for various resolutions in Figure 12. It is clearly observed that in this mass region a mass resolution of 5000, typical of standard high-resolution separators, provides essentially no purification. At a resolution of 10000 one observes a structure in the mass spectrum that clearly indicates the presence of the different isobars and it is only by the time one reaches mass resolution of 20000 that one obtains good beam purity at high transmission.

This essentially sets the mass resolution that the isobar separator must achieve for our purpose. Aiming at higher resolution yields only small gains at the cost of higher technical difficulties and cost.

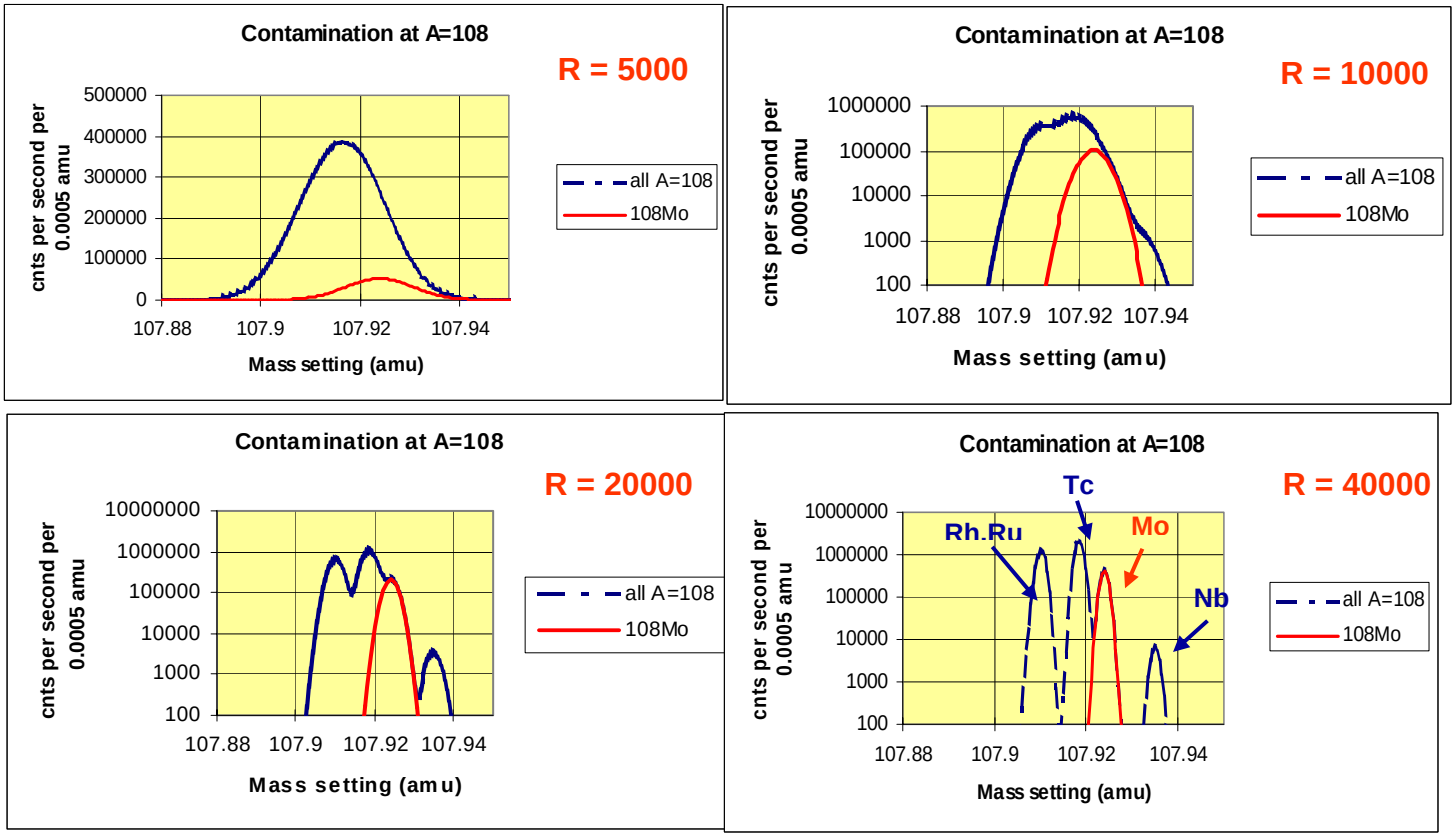

Figure 12. Mass spectrum observed for A=108 isobar at various mass resolving power. It is clearly seen that in this mass region a mass resolution of 5000 provides very little isobaric selectivity and that about 20000 resolution is required to obtain a high degree of purification.

The second critical input is the beam properties expected out of the gas catcher/gas cooler system. These properties are actually excellent since the gas cooler cools the ion beam to the temperature of the gas and small transverse emittance ($< 3\pi$ mm mrad at 50 keV) and

energy spread are obtained for the nA ion currents we will run through the device in this application. The presence of the gas cooler required to remove the ions from the high pressure region is ideal for this application as is demonstrated by the fact that numerous ISOL facilities have plans to incorporate RFQ gas coolers in their system to improve the ion beam properties of their standard ISOL sources.

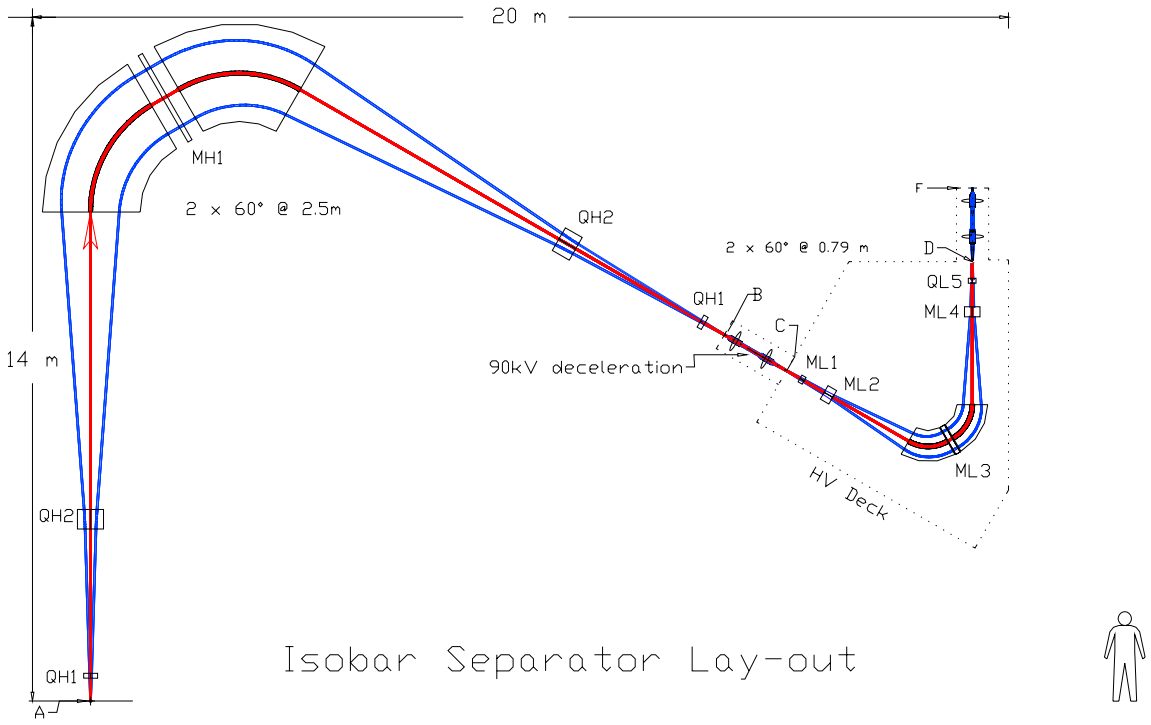

Figure 13. Layout of the two-stage isobar separator designed for RIA. The lower transverse emittance and energy spread obtained from the gas cooler allow one to obtain the required resolution with a scaled down version of the first half of this separator.

An isobar separator capable of obtaining the required mass resolution with standard ISOL beam emittances has been designed recently at Argonne [11] for the RIA facility (see Figure 13). It utilizes a two-stage concept to eliminate the effect of energy spread in the beam. The first stage has a large dispersion and yields a mass resolution of 22000 for a 10π mm mrad transverse emittance at 100 keV. The beam is then decelerated to 10 keV

and passed through a second stage with a dispersion and radius scaled down by the momentum ratio with respect to the initial stage. This second dispersion cancels out the effect of the energy spread on the first dispersion (smaller dispersion but with proportionately increased momentum spread) while only decreasing the total mass resolution by 10%. The result is an overall mass resolution of 20000 for a 10π mm mrad transverse emittance at 100 keV and an initial energy spread of ± 10 eV. This ambitious design can achieve high resolution with a much poorer quality beam compared to similar devices, but at the cost of a footprint of 14 meters by 20 meters.

This isobar separator is much too large to fit on a high voltage platform but the normalized emittance of the beams that will be extracted from the gas cooler system will be a factor of 4.7 times smaller than those for which the RIA isotope separator was designed. This implies that scaling down the first section of this separator by a factor of 4.7 to a radius of 0.53 meter would yield a mass resolution of 22000 similar to that of the first section of the RIA isobar separator if no energy spread is present. The gas cooler beam energy spread of less than 1 eV does not require a second stage for correction as long as the total accelerating voltage is above 44 kV. The design that has therefore been judged optimal for the present application is to use an ion optics similar to that used in the first part of the RIA isobar separator, but scaled down by roughly a factor of 4 to a bending radius of 0.6 meter. The bending angle is still 120 degrees with two 60 degrees bending magnet separated by a multipole element to correct for aberrations. With a total acceleration voltage of 50 kV, this yields a mass resolution in excess of 20000 with slit size of 0.25 mm. This fulfills our performance requirements with the gas catcher, isobar

separator and focal point all fitting on the gas catcher high voltage platform. The main technical requirements to achieve this resolution are the homogeneity and stability of the magnetic field integral across the magnet poles and the high voltage stability. Both are well within performance level that have been achieved by other devices in the past.

F. Beam dump

One important consideration for the operation of the upgrade within ATLAS is to minimize the spread of radioactive contamination outside of the gas catcher high voltage platform. Essentially all activity extracted from the gas catcher will be transported to the isobar separator and then dispersed in its focal plane with a dispersion of just above 5 meters. A movable slit assembly at the focal plane will let the mass of interest go through and stop the isobars and neighboring masses. The assembly will also include a wire scanner (with current read out at normal beam intensity and secondary electron detection at very low intensity) to tune the isobar separator. The full assembly must be shielded and serviceable. In addition, isotopes of masses further away from the mass of interest will be implanted on liners surrounding the beam envelope in the dispersive plane. These liners should be removable (and possibly disposable) for servicing of the isobar separator. The gamma activity collected on these liners will be shielded by the magnet themselves and thin additional shielding outside if required. Thin high-Z shielding around the vacuum chamber leading to the focal plane will be used to deal with the gamma activity from the accumulated fission fragments.

G. High voltage platform

The injection of the radioactive ions into the charge-state breeder requires that the potential at which the gas catcher is operated be the same as that of the plasmas in the ECR breeder. The potential of the ECR-1 high voltage platform is set by the acceleration in ATLAS which requires up to about 250 kV of acceleration before injection into the PII linac for the heaviest of the beams considered in this upgrade. The ECR source is typically operated at 15 kV above the ECR platform voltage to enable beam formation before the magnetic analysis in the 90 degrees magnet on the platform. On the gas catcher high voltage platform, the isobar separator magnet and optics need to be sitting at 50 kV below the gas catcher potential. For optimum operation, the isobaric separation sets a requirement for the 50 kV between the gas catcher and the isobar separator system to be stable at the one volt level.

Similarly, for optimum capture in the ECR plasma, the few volts difference between the gas catcher and the ECR breeder potentials must also be stable at the volt level. These requirements are best met by monitoring or comparing the smallest voltage differences possible; this yields higher precision and minimizes the potential for over-voltage across electronic equipment. It was therefore decided that the gas catcher high voltage platform would be tied electrically to the ECR-1 high voltage with a low voltage power supply that will be used to fine tune the difference in potential for optimum trapping in the charge breeder. The low-voltage supply will be properly protected against overvoltages. The gas catcher and gas cooler system will be tied to the high voltage of the platform. This

eliminates the possible influence of voltage ripple on separate high voltages. The isobar separator section on the gas catcher platform will be biased by a –50 kV supply with respect to the gas catcher potential. The beam will then be de-celerated to the source platform voltage as the beam transitions from the gas-catcher platform to the charge-breeder platform. These voltage and energy relationships are shown in Figure 16. This high-voltage will be measured absolutely and locked by feedback from a high-precision temperature-stabilized high voltage divider. These relationships between the different voltages minimize the potential for the destruction of sensitive equipment in the case of failure of any component. The two physical platforms will be at a potential difference of roughly 15 kV that will allow for a relatively simple transfer section between both. The high voltage power supply biasing the ECR source will provide bias to the gas catcher platform and gas catcher. Electrical power for the gas catcher and gas cooler electronics and pumps on the new platform will be provided by a 300kV 100 kVA isolation transformer. A second smaller isolation transformer rated for roughly 30 kVA at 50kV, referenced to the platform, will provide power to the isobar separator magnets and related equipment. All connections between the two platforms will be removable to allow operation of the ECR-1 source in a standalone mode and for beam development from the fission source separately from injection into the charge state breeder.

The gas catcher platform will have a size of 20 ft by 14 ft, similar to that of the existing ECR platforms. It will be located 8 ft away from the ECR-1 platform. An independent cage will be built adjacent to the existing cage surrounding the ECR-1 platform to host the new platform. The links and transfer line between both platforms will pass through

the wall separating the cages. By removing these connections, the two cages/platforms will be able to be operated independently. A schematic view of the gas catcher platform and its equipment is shown in Figure 14. The gas catcher, gas cooler, isobar separator, shielding and related equipment all must be accommodated with most components isolated and biased with respect to the platform. The total weight on the gas catcher platform is significantly higher than on the existing ECR platforms, but is not difficult to handle. We use commercial high-voltage transmission system 'station posts' as insulating legs. Each leg is rated for a compressive load of 12.5 tons, but is recommended to be designed for half that value. Thus the twelve legs used on ECR-I are capable of a design load of 75 tons, far in excess of the total weight of the all items planned for the new platform. Therefore the construction technique and the supporting insulators can be similar to those used previously with some additional strength added to the steel superstructure.

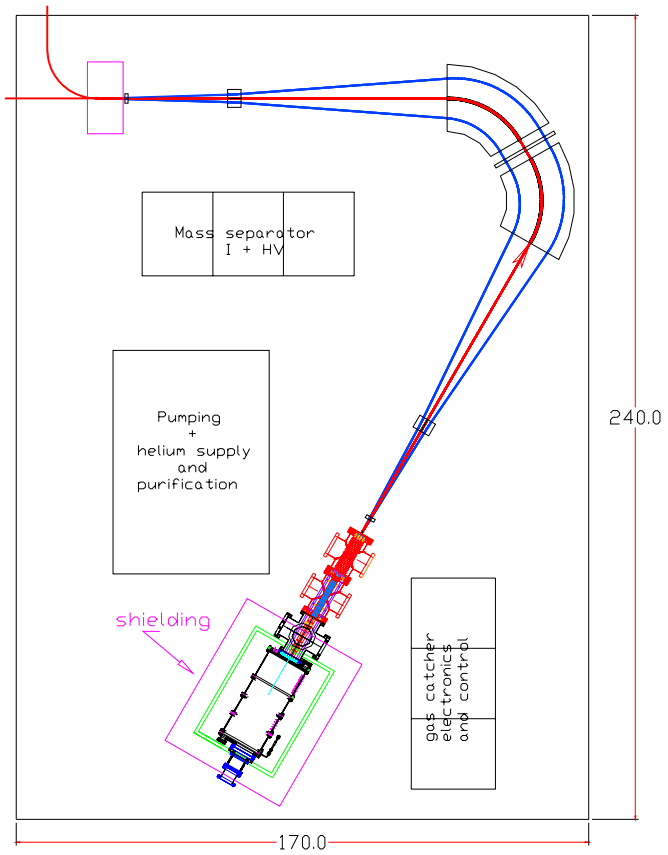

Figure 14. Schematic layout of the gas catcher, gas cooler, shielding, isobar separator and related equipment on the gas catcher high-voltage platform.

H. Source region transport system and unaccelerated beam transport

The transport system will take the selected activity from the output of the isobar separator and deliver it either to the charge-state breeder on the neighboring high voltage platform or to a diagnostics station off the platform at ground potential. The transport for these low energy beams is performed with electrostatic steering and focusing elements. This allows the beamline tuning to be mass independent. An acceleration column is required on the section leading to the diagnostics station. Diagnostics along the transport system must include Faraday cups for the highest intensity beams, beam profilers that can operate with low intensity beams and beta detectors to monitor activity. See section "K" below for a discussion of the diagnostics required for transport to the ATLAS accelerator and on to the experimental stations.

I. Diagnostics station

Tuning of the gas catcher/gas cooler/isobar separator ensemble must be optimized to obtain maximum yield. The multi-parameter space requires proper diagnostics. Clear identification of the isotopes is critical. This can be achieved with a tape station, a high efficiency beta counter and a gamma ray detector. By collecting the activity for a fixed time and moving it in front of the beta detector one can determine the total radioactive beam intensity and measure the decay lifetime which identifies the dominant isotope and contaminants. Additional information can be obtained when needed from gamma ray identification. The accumulated activity is removed by the tape transport system after

each measurement cycle allowing for clean conditions for each new measurement. The cycling time is typically fast enough to allow tuning of the extracted yield with the beta detection as "live" diagnostics.

In addition, part of the physics program envisaged for this upgrade involves study with stopped or low energy beams of radioactive ions. The diagnostics station will receive such beams at the full ion source intensity, independently of the rest of the ATLAS accelerator. An electrostatic switchyard in front of the diagnostics station will allow other more specialized detection systems to receive the beams of interest for these low-energy studies.

J. Charge state breeder

Over the past eight years a variation on a standard ECR ion source, known as the charge-breeder ECR ion source has been developed, largely led by groups in Grenoble [6]. This work is based on the realization that the plasma potential, formed in the central region of a standard ECR ion source, can be used to capture low charge-state injected ions and then subsequently ionize those captured ions further by electron bombardment in the plasma. This capture process is possible only if the incoming ions are near to the source axis, to avoid reflection of the ions by the magnetic mirror, and if the ions can be slowed to energies below a few eVs, to allow capture by the shallow plasma potential. Capture of the ions is required since the ions must be trapped for 10-100 ms in order to strip them to

high charge states. Single passage transit times across the source are a small fraction of this stripping time so the ions must be confined for many equivalent transit times.

The precise beam properties required for capture into the charge breeder are not well defined, but energy spreads of 2-4 eV and transverse emittances of <100π mm*mr are needed typically for good capture. Lower emittance beams should be helpful for injection through the mirror by minimizing mirror reflection from angular momentum conservation. The beam properties of the fission fragments emerging from the helium gas catcher are expected to exceed these general requirements and therefore are expected to be efficiently matched into the charge breeder.

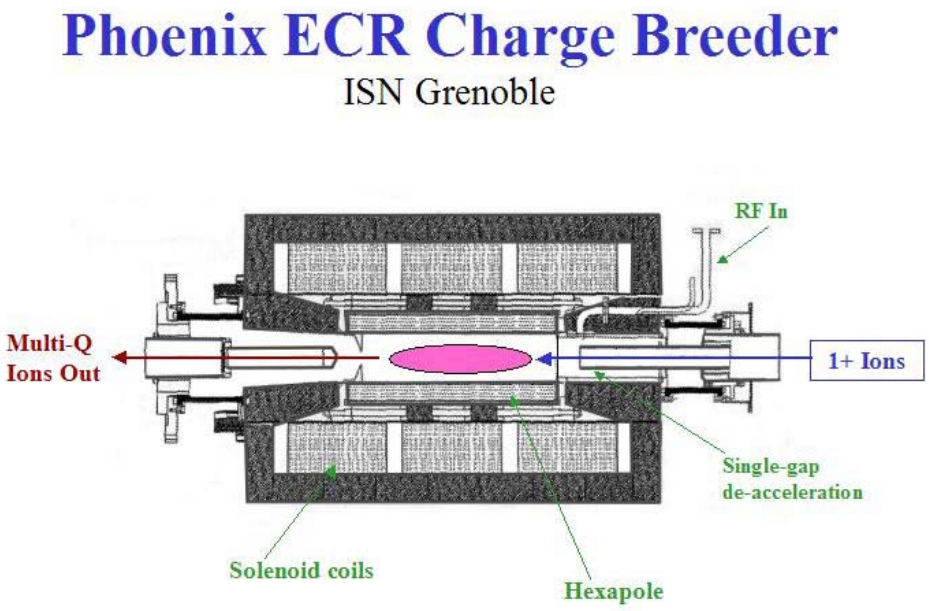

Figure 15. Cross-section view of the Phoenix ECR charge breeder.

A cross-section view of a charge-breeder ECR source is shown in Figure 15. The major modifications to convert a standard ECR source into a charge breeder source are to provide the necessary opening and beam optics into the plasma regions for delivering the

1+ ions. The injection optics for the low charge-state seed ions must maintain good beam focus as the ions traverse the high magnetic field mirror region to avoid reflection from the field. The final deceleration must be accomplished as near to the plasma as possible to minimize beam blowup. Once deceleration occurs, the final capture into the electrostatic trap occurs through ion-ion collisions scattering the low-velocity ions into the potential well.

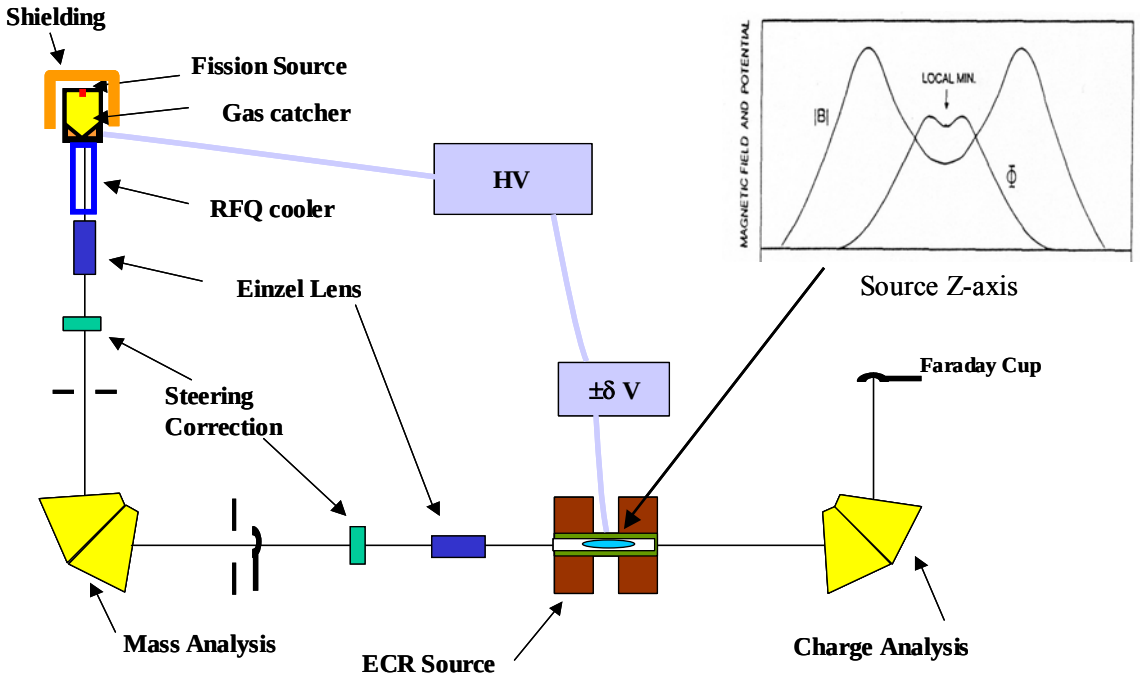

Figure 16. Schematic view of the transfer of activity from the gas catcher to the ECR charge state breeder.

Because the trap is so shallow, the beam deceleration must be extremely precise. In Figure 16, the overall beamline configuration between the fission source and the charge breeder is shown along with the beam control and voltage biasing elements. One sees that the fission source system and the charge breeder must be placed at the same voltage

except for a small voltage difference which modifies the charge breeder voltage by a few volts. This provides the energy flexibility to allow the 1+ or 2+ ions to be trapped in the electrostatic well.

The efficiency of converting 1+ or 2+ ions into n+ ions varies significantly with the species considered. For gaseous species, recycling from the walls improves the total efficiency for stable ion beams by approximately a factor of 2 compared to condensable materials. For radioactive beams, this enhancement may not be so significant since the total time from injection to extraction will be lengthened by the wall recycling. For stable beams, the best efficiencies observed to date are shown in Table 2 below. The efficiencies for radioactive beams will be reduced due to the latency time in the source compared to the species lifetime. Most species populated strongly by californium fission have lifetimes of seconds or more and will not be affected, but the weakly produced isotopes with lifetimes significantly shorter than 100 ms will be noticeably attenuated by decay.

Table 2. Table of measured ion efficiencies achieved in charge breeders. Data are from references [7,8,14].

	Efficiency	A/Q	Time(ms)
Gases			
$^{40}Ar^{9+}$	11.9%	4.4	25
$^{84}Kr^{14+}$	10.3%	6.0	60
Solids			
$^{115}In^{18+}$	6.0%	5.8	
$^{109}Ag^{19+}$	3.9%	5.7	25
$^{120}Sn^{22+}$	4.0%	5.5	20(19+)

For this project, we plan to modify the existing ATLAS 10 GHz ECR-I source to function as a charge breeder. A cross-section view of the present ECR-I is shown in Figure 17**.** The modifications required for ECR-I are focused on the 'injection' end of the source, the normal location of material feeds, biased disks, RF waveguide, and other diagnostic and utility function. These components will be rearranged to allow a one or two stage deceleration electrode assembly to control the 1+ beam as it decelerates to a near stop. A preliminary design of the modified ECR-I source is shown in Figure 18.

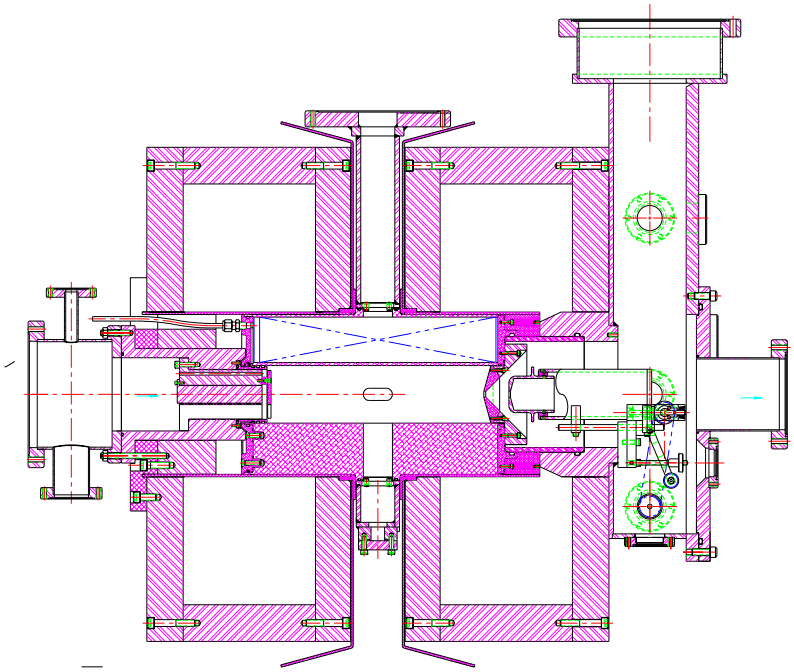

Figure 17. Present ECR-I 10 GHz Ion Source

For most cases, long-term contamination of the interior of the source will be rather modest. The longest-lived species directly produced by the fission of ^{252}Cf is ^{144}Ce (284.6d) and is produced with rather low intensity (2.7E+5 s^{-1}) while the next longest lived species is ^{140}Ba (12.75d) produced at a rate of 1.4E+6 s^{-1}. About half of those will be lost in the ECR source and at saturation they correspond to total radiation levels of

1.4 mrem/hr and 15 mrem/hr respectively at 30 cm, if concentrated at one point rather than distributed over the interior of the source. Similar radiation levels are reached with the long-lived daughters of shorter-lived isotopes with the total decay rate never exceeding the activity deposition rate so that the maximum activity level that could be expected is about 100 mrem/hr for an isotope with a week lifetime along the decay chain. Generally speaking, maintenance-requiring access to the interior of an ECR source is rare, but it does occur. Even though the level of activity requires only careful monitoring and maintenance procedures, it may be desirable to install a liner in ECR-I to allow easy cleanup of the source and do necessary maintenance. ECR-I has operated in the past successfully with a stainless steel liner and we see no significant issues with using such a liner when deemed necessary. But in general we do not believe this will be necessary.

The injection beamline from the mass separator to the charge breeder will consist of a 90 degree bending magnet and electrostatic focusing lenses to match the radioactive 1+ beam into the source. Beam current and beam size diagnostics, using secondary electron emission and MCP detection, will be mounted at the image point of the analyzing magnet, just ahead of injection into the source. A simple blocking shield will protect this sensitive electronics from beam leaking from the operating ECR source. In order to provide the necessary space for a 90 degrees bending magnet as part of the beam transport from the fission source to the charge-breeder, ECR-I will be moved up to the entrance waist point of the extraction beamline analyzing magnet. This configuration has been employed already at a number of ECR source facilities throughout the world and so should pose no serious concerns. In fact, such close geometry is an improved design

from a space charge concern (keep in mind that the source will run mostly on support gas and so space charge effects near the source extraction region are a significant issue).

The development of the charge breeder source will need to progress in parallel with the gas catcher fission source development. Although the physical changes needed to convert ECR-I to a charge breeder are relatively modest, significant development work such as learning how to optimally operate an ECR source as a charge breeder will be required. A separate stable-beam 1+ ion source will be used to develop the proper operating modes for the source. We estimate that a full man-year of effort from the existing ECR group is necessary to implement the design changes and to undertake charge breeding studies during the 2 years of this project. This would be followed by the permanent expansion of the group by one person to continue operation and development.

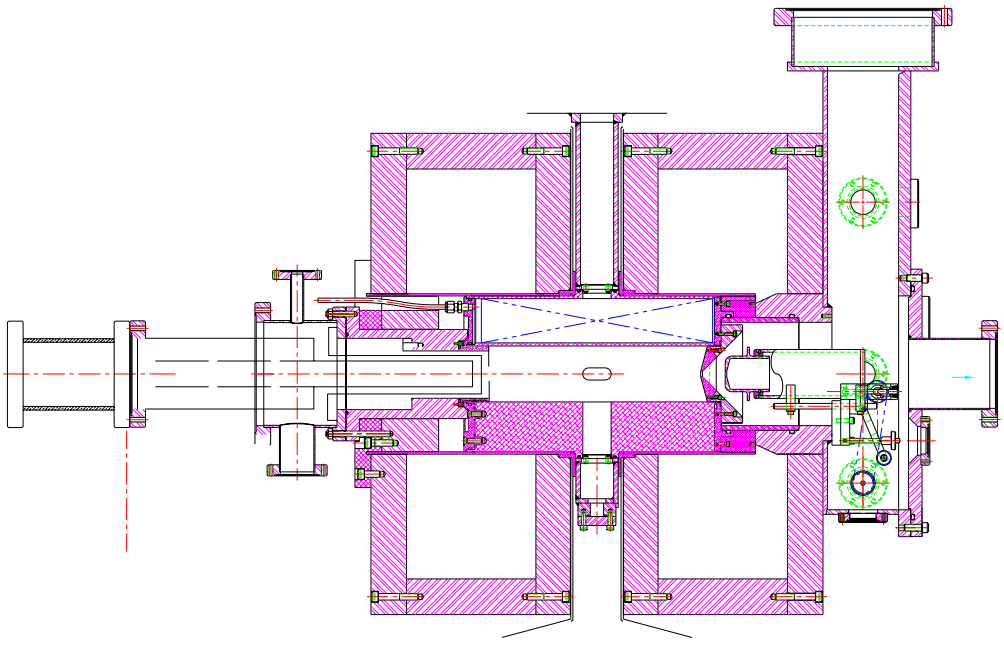

Figure 18. ECR-1 modifications required for charge-breeder operation.

The modifications required for ECR-I may affect the charge-state distribution slightly, but otherwise the source can continue to operate as a stable beam source as well as a charge breeder. But once construction begins, which will take only 4-8 weeks, then commissioning of the source as a charge breeder will require a focused effort. Therefore the source will not be available for at least six months after the modifications to allow these development efforts. Initial work will be with stable beams from simple 1+ ion sources such as surface ionization sources. Then once the fission fragment system is commissioned, additional development time will be necessary to learn how to best operate the total system. Thus during the second year of construction, ECR-I will be available for stable beams operation with ATLAS on a very limited basis. Once fully commissioned there will continue to be some development effort, but at this point ECR-I will return to being schedulable for stable as well as radioactive beams.

K. ATLAS and diagnostics improvements

ATLAS operations has considerable experience with low-intensity beams. Programs with radioactive beams, such as ^{18}F, ^{56}Ni, ^{56}Co, and with accelerator mass spectroscopy (AMS) have required the development of techniques for acceleration of beams with little or no diagnostics possible. In general the accelerator is tuned with a 'guide' beam, that is a beam with nearly the same charge-to-mass ratio (q/m) as the weak beam of interest. A small scale factor is then applied to that tuned condition to provide the required tune for the weak beam. Reliance on the researcher's detection system has been important up to now in optimizing the tune configuration.

This general approach will still be the primary method of accelerator setup for these fission fragment beams, but additional weak-beam diagnostics will be needed to provide a more flexible, and experiment-independent tuning algorithm. Low-intensity profile monitors have been developed as part of the RIA activity and will be added to the ATLAS diagnostics system to provide both beam profile information and beam current measurements. These profile monitors will also serve as Faraday cups at those locations. To reduce costs other ion counters ("Faraday cups") will be installed at other locations in the beam transport system. The costs for these systems included in the budget assume that only the beamlines to the spectrograph, FMA, Gammasphere and (hopefully) the proposed solenoid spectrometer will be developed initially as part of this construction project. More stations can be implemented later as demand warrants. The low-intensity diagnostics stations necessary for this configuration are shown in Figure 20.

ATLAS uses silicon solid-state detectors systems routinely for beam tuning by elastically scattering the primary beam at small forward angles in order to measure beam energy and time. These systems will be modified to allow insertion at zero degrees, which in combination with attenuators will allow direct observation of the radioactive beam properties. Later, development of high-pressure gas detectors and other detector systems will be pursued. This work is not necessary to the successful completion of this project but is seen as part of ongoing improvement efforts that are a natural part of any operating facility. Funds for this effort would be expected to come from the facility operating and capital equipment funds.

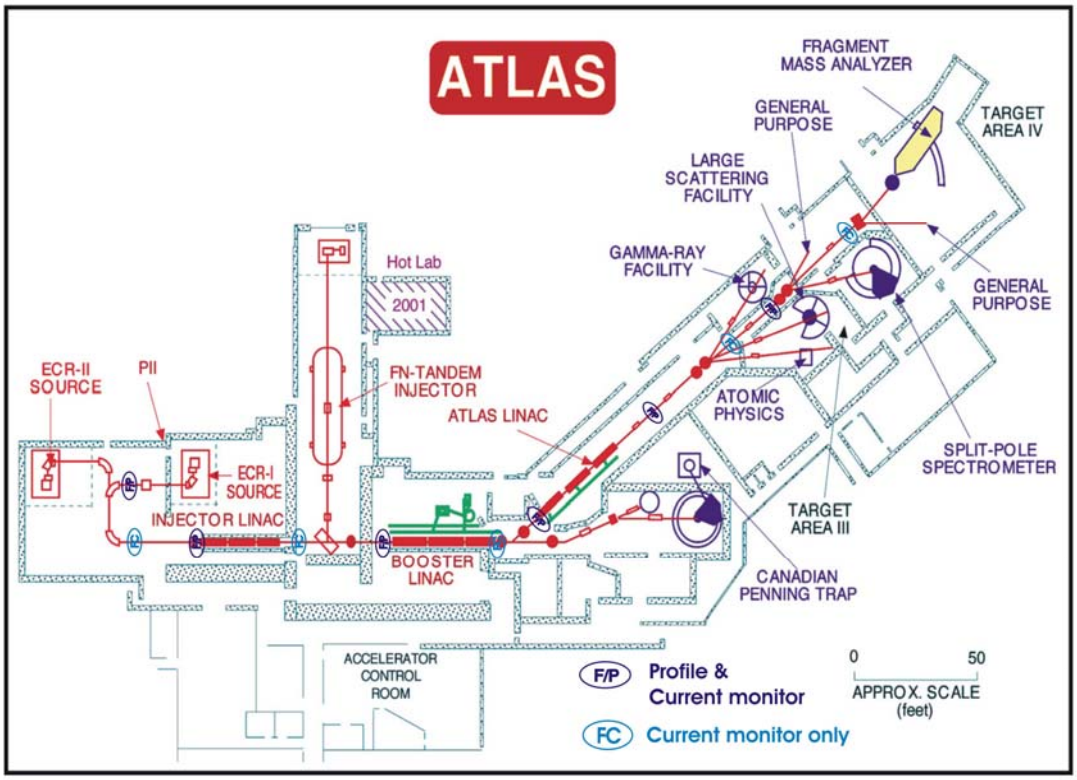

Figure 19. ATLAS floor plan showing the planned locations for low-intensity profile monitors and beam current monitors. This plan assumes beam delivery to four target stations.

Finally, the transmission through the accelerator system must be optimized. ATLAS itself, with its large acceptance superconducting cavities, is a very high transmission accelerator. The only expected limitation to the transmission is due to the theoretical limit of 85% efficiency for the multiharmonics buncher and the 90% transmission of the buncher grids. In everyday operation at ATLAS, the beam current delivered to experiments is usually limited by what targets can tolerate or by administrative radiation limits. Work is underway to improve the transmission in the low-energy beam transport section from ECR-I to PII. We believe presently achieved transmission of around 70% from ECR-I can be improved significantly. Costs for this activity are not part of this project, but are rather viewed as routine on-going accelerator development.

VI. Operation Issues

ATLAS is the premier low-energy stable beam accelerator in the US. It serves a large community of users and it is important that the implementation of this upgrade does not result in a significant increase in down time for the facility. The connection of the radioactive beam ion source to the ATLAS accelerator is only through the ECR-1 ion source. The ECR-2 ion source operation is not disturbed by the upgrade and will be used for experiments requiring high beam intensity. ECR-1, after its modification to a charge breeder, will remain operational as an ECR source in standalone mode. The installation of the gas catcher high voltage platform in an independent cage allows it and the ECR-I high voltage platforms to be essentially independent during construction or while low-energy experiments are performed out of the gas catcher platform. As a result, the current flexibility and low downtime available with two sources for stable beam operation will be maintained. The ability to operate and tune the gas catcher and isobar separator independently from the rest of the facility is a distinct advantage. The connections between the gas catcher and ECR-1 platforms will be installed only for experiments with accelerated neutron-rich beams. Tuning of the capture of the radioactive beam into the charge breeder can be performed while a stable beam experiment is running out of the ECR-2 source, in a fashion similar to the development of stable beams in ECR-1 while experiments are running out of ECR-2, a procedure frequently used today. High-voltage relationships between the different components are also such that the ECR-1 voltage can be varied to optimize transmission through the

accelerator without modifying the voltage relationship between ECR-1 and the gas catcher so that injection into the charge state breeder does not have to be retuned. Similarly, tuning on the gas catcher platform will not require retuning of ATLAS. The upgrade will provide beams that would normally be obtained with the two-accelerator method (one to produce the activity, one to post-accelerate), but will require running only one accelerator. The only significant difference on the schedule will then be the longer expected tuning time for the accelerator because of the lower beam intensities. Because of the high efficiency of the overall facility, the total inventory of radioactive material is kept to a minimum and the radioactivity that can be lost inside the accelerator (see section VII) is not high enough to warrant modifications of the maintenance and repair procedures now in place.

VII. Safety Issues

The proposed ATLAS californium upgrade increases the radioactive beam capabilities at ATLAS by adding a source of short-lived neutron-rich isotopes to the facility. This addition does not change the classification of the ATLAS facility since the threshold for a category 3 nuclear facility is 3.2 Ci of ^{252}Cf according to DOE Std. 1027-92. (The Physics Division does maintain a 100 milligram Pu-Be neutron source that will need to be placed in a special isolation container so that the Division does not exceed a Category III facility.) A significant revision to the ATLAS Safety Assessment Document will be required to address the new hazards and changes in facility configuration. In addition

new operating procedures and additional training for the ATLAS staff will be required to ensure safe operation of the facility.

Most changes to the facility will be on a new high-voltage platform that will host the gas catcher containing the high-intensity fission source and some low-energy beam preparation equipment. Two high-voltage platforms are in operation at ATLAS for the existing ECR sources and the required safety procedures, including a number of redundant grounding procedures to allow access to the platforms, are in place. There are additional electrical hazards associated with the operation of a large gas catcher which have also been dealt with before at ATLAS. Safe procedures for the standard operation of the new device, based on engineering controls, administrative controls and proper training, will be devised based on this expertise. Those procedures will undergo independent safety reviews during the project, and be approved by the safety authorities at Argonne before operation. These are standard procedures at ATLAS for any new major piece of equipment.

The californium upgrade project also introduces a significant potential hazard with the presence of a 1 Ci ^{252}Cf source that raises issues of shielding and possible contamination. All fissionable activity and the bulk (>99%) of the radioactive fission products will be confined to the gas catcher high-voltage platform. Simulations and reports from other facilities indicate that the 1 Ci fission source, unshielded, would yield a neutron radiation field of just over 4 rem/hr at 1 meter and a gamma field of 250 mrem/hr at the same distance. ATLAS can generate similar radiation fields, but those disappear when the

accelerator is turned off; with the fission source they remain until the source has decayed away. ATLAS has expertise with sources of that magnitude in the existing research program with radioactive beams, but these are generally shorter-lived beta-emitters (^{18}F sources used in the past had strength of up to 1 Ci) that emit no neutrons. Argonne has expertise and facilities capable of dealing with sources of neutron emitters of this magnitude. The main radiation safety tasks are to ensure safe preparation, transport and installation of the source without introducing contamination, and proper shielding and containment of activity during operation and maintenance. The transport cask and installation mechanism have been described earlier, the calculations used to determine the required shielding are briefly described below.

A first estimate of the required shielding was obtained by requiring a total radiation field at 30 cm from the shielding surface of about 1 mrem/hr. Using the MCNP code and a proper description of the source, we obtained for a spherical geometry and shells of 5 cm of steel, 60 cm of 5% borated polyethylene and 5 cm of lead fields of 0.3 mrem/hr neutrons, 0.2 mrem/hr gamma (from the neutron capture), 0.6 mrem/hr gamma (direct), for a total of 1.1 mrem/hr at 1 meter from the source (30 cm from the shielding). These numbers essentially set the requirements for the cask used for the transport of the source and for the permanent shielding on the sides of the gas catcher.

For a more detailed understanding of the shielding required, especially at the entrance side of the gas catcher where the source will be inserted, the geometry shown in Figure 20 was investigated. A particular concern was that the shielding permanently present

around the gas catcher be sufficient to allow access for limited time periods to the vacuum sealing port used to bring in the source. As shown above in section III.C, the cask is in place during the installation of the source and vacuum sealing, and remains in place after installation to provide additional shielding. If the sealing mechanism were however to get stuck, manual intervention might be necessary. Under these conditions and with the shielding shown in Figure 20 (3/4" steel, 10" borated polyethylene and 2" lead), the radiation levels one would be exposed to working on the sealing would be 137 mrem/hr neutrons, 1.5 mrem/hr gamma from capture and 10 mrem/hr gamma direct for a total of 150 mrem/hr at 30 cm from the accessible surface. This would make such emergency repair operation possible. In addition, for this critical back region that we would like to remain thin, a new shielding material made of a mixture of Colamenite and Epoxy resin could be used instead of borated polyethylene to reduce the radiation fields further by about a factor of 2. This possibility is being investigated.

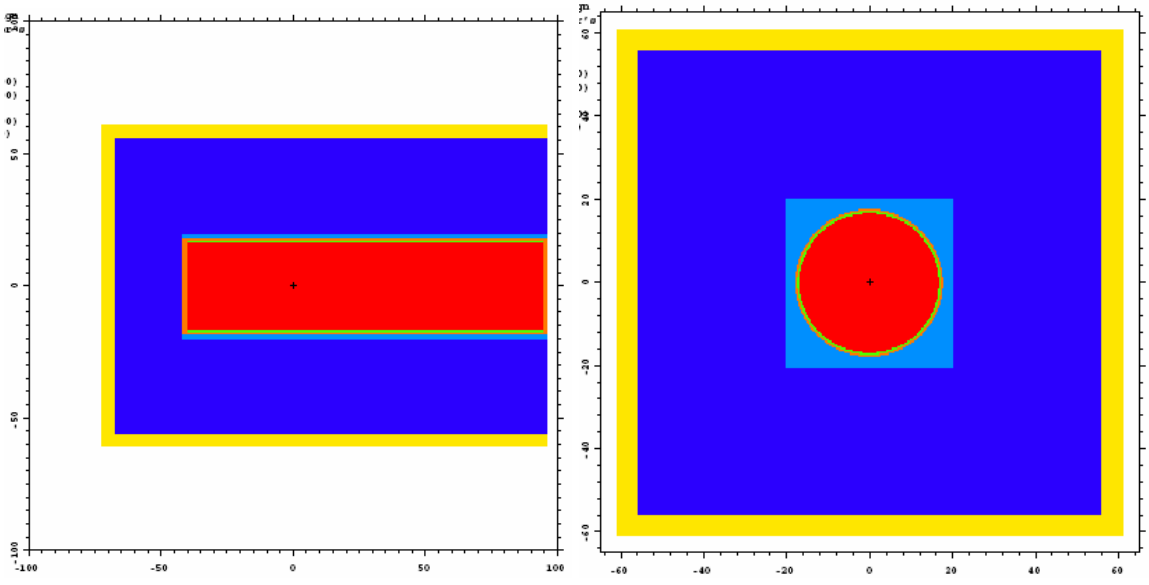

Figure 20. Views of the geometry used in the radiation calculations with the MCNP code. The color coding is: Red – helium gas, Orange- steel, Green – aluminum, Blue – borated polyethylene, Yellow – lead. The source is located on the axis and at the back of the gas catcher.

For all other gas catcher repair or maintenance operations, the source would be retrieved into the cask that would then be closed. The only radioactivity left to be dealt with in this case is that from the fission fragments accumulated in the gas catcher. After months of operation the inside of the gas catcher would reach levels of about 5 rem/hr of low energy betas and 30 mrem/hr of gammas. The low energy betas are easily shielded from but the gamma field is a more serious concern. To alleviate this difficulty it was decided that the gas catcher design has to be highly modular so that sections could be easily removed and replaced in cases where major maintenance or repair is required. A complete spare would be available and the appropriate spare section would replace a failed one. This failed section would then be transported to a hot lab for repair or packing for disposal, if necessary. It is likely that maintenance requiring only a few hours total work might be possible without removal and spare replacement.

During these maintenance activities, the vacuum system will be opened and thus made common with the general room. The maintenance activities make the possibility of spreading contamination out into the space around the gas-catcher beamline a possibility. It will therefore be necessary to create an isolation 'room' around this maintenance area, complete with a HEPA-filtered air system, radiation monitors, and other standards for a contamination area. It is proposed to use a temporary "tent" to define the area. The structure will involve a permanent metal frame on which tent-like walls will be attached, creating an isolated space. During normal operation some of the tent walls will be rolled up providing easy access to the platform region. When it is required to open the vacuum

system and therefore create the possibility of contamination, the tent walls are closed, and a HEPA filtration system installed to filter and exchange the air in the tent. Such a system has been designed by ANL Waste Management personnel. The estimated costs of the tent system is less than $5000. The entire maintenance operation is then monitored by Waste Management and ESH personnel. Disposal of any contaminated components, up and including the entire gas catcher assembly in a worst-case accident, will be handled by ANL Waste Management personnel. For such a worst-case accident requiring disposal of the fission source, its cask and the gas catcher, the estimated cost is $100,000 but no significant spreadable contamination is envisioned even under this worst-case scenario.

Radiation levels in the gas catcher area will be monitored at all time by neutron and gamma monitors interfaced to the ARIS radiation monitoring system currently in use at ATLAS. Any operation that requires opening the vacuum system around the gas catcher or working for extended periods of time on the platform will be monitored by health physics personnel once the proper radiation work permit for the intervention has been granted.

Most radioactive ions not extracted as beam from the gas catcher will coat the walls of the gas catcher except for the neutrals from volatile species such as xenon and krypton that will be extracted and pumped out in the first section of the RFQ cooler. The pump exhaust will go through an HEPA filter that will remove most contamination while the inert species (such as radioactive xenon isotopes that will be present at the 10^7 atoms per

second level) will be released. These noble gases do not present a health risk and are considered safe to exhaust. Of course an annual report of our releases is required and that is handled by the Laboratory ESH support groups.

The radioactivity that will reach other components of the facility is much smaller in magnitude. Of the order of 10^7 radioactive ions per second will be transported to the ECR-1 high voltage platform and injected into the charge state breeder. Activity build up of up to a few hundred μCi will occur after long periods of running. Removing the breeder liner should eliminate radiation exposure and allow normal maintenance on other components on that platform. The beams sent through the accelerator for post-acceleration will have intensities of up to 10^6 particles per second. A beam dump collecting the full beam intensity for a week would accumulate roughly 25 μCi of short-lived activity that would then decay over time. This activity is not beyond present levels experienced at ATLAS with high intensity stable beams on thick targets. Losses along the beamline will be minimal and the activity accumulated at these points will scale accordingly. No additional precautions or procedures besides those currently in place are expected to be required along the accelerator and beamlines for the radioactive beams.

The radioactive wastes generated by normal operation and maintenance (such as the HEPA filters) will be handled in a fashion identical to how such wastes are handled now at ATLAS. Every component removed from any experimental area at ATLAS is treated as low-level radioactive waste that is dealt with at fairly low cost by the existing infrastructure. It is not expected that the total amount of such waste will be significantly

changed by the upgrade. Even the components in direct contact with the californium source would fall in this category since the lifetime of californium is too short too fall under the transuranic waste category.

Finally, the very effective containment of most radioactivity to one high-voltage platform will minimize the eventual decommissioning costs. Essentially all accumulated radioactive inventory will be inside the gas catcher and the vacuum vessel and beam dump of the isobar separator. There will be some additional contamination in the transport cask and, to a smaller degree, in the liner of the charge state breeder. We expect no changes to the status of the remainder of ATLAS, and as a result, no changes to the decommissioning costs of the bulk of the ATLAS facility.

VIII. Budget

The proposed ATLAS californium source upgrade is based in large part on technology developed and already in use at Argonne and, as a result, for most components we have recent purchasing or fabrication cost information available. These costs have been escalated for inflation where necessary. Engineering designs and production of machine drawings will be carried out in the Physics Division. Fabrication of these custom designed components will be done by Argonne or commercial vendors depending on costs, time scales and quality assurance considerations. The estimated costs of individual sub-assemblies are listed in Table 3. The contingency associated with each budget item varies between 10% and 30%, depending on the uncertainties associated with individual

costs. Assembly and testing will be carried out by a combination of Physics Division staff members and additional personnel whose support is requested within this proposal. Overhead rates are estimated based on the rates which apply at Argonne National Laboratory during FY2005. The overhead rate on procured items is 9.2%, whereas the rates on laboratory services varies between 22.6% and 29%.

Table 3. Cost distribution for ATLAS californium upgrade project.

item	cost ($k)	contingency (%)	total cost ($k)
room preparation			
move test cryostat facility	20.0	20	24.0
provide cryogenics (liquid helium and nitrogen)	125.0	20	150.0
miscellaneous wiring and improvements	25.0	10	27.5
ECR1 platform modifications			
ECR source modification	70.0	30	91.0
injection beamline vacuum system	41.5	20	49.8
lens	15.0	20	18.0
90 degree magnet into source	40.0	10	44.0
HV platform			
Platform Design	7.4	10	8.1
Support Legs	8.9	10	9.8
Platform construction & materials	111.0	10	122.1
HV Transformer (300kV, 100kVA)	70.0	10	77.0
Chilled water	50.0	10	55.0
Electrical installation	29.6	10	32.6
Radiation control & monitoring System			
Detectors gamma & neutron (4)	24.0	10	26.4
Enclosing cage (install. Incl.)	10.0	10	11.0
Incorporation into ARIS	25.0	10	27.5
HV safety interlock system	15.0	10	16.5
HV stabilization between platforms	10.0	20	12.0
gas catcher and support structure			
gas catcher cone section	25.0	20	30.0
gas catcher body sections (3)	24.0	20	28.8
gas catcher body sections (spare)	8.0	20	9.6
gas catcher nozzle	0.5	20	0.6
gas catcher entrance plate	2.5	20	3.0
gas catcher seals	4.0	20	4.8
support structure	3.0	20	3.6
all-metal bypass valve	2.0	10	2.2
heater system	1.0	10	1.1
gas cooler			
RFQ structure (2)	10.0	20	12.0
vacuum chamber (2)	4.3	10	4.7
fission sources (procurement and shipping)	33.0	20	36.6
source handling / contamination containment			
shielded cask, scissor lift table, automation	100.0	20	120.0
hot cells refurbishment	30.0	20	36.0
electronics for gas catcher/cooler			
low voltage DC supplies	3.5	10	3.9
high voltage DC supply	4.0	10	4.4
RF generators (4)	10.0	10	11.0
RF amplifiers 50W (3)	19.5	10	21.5

RF amplifiers 150W	8.0	10	8.8
RF power tune circuit and distribution	1.5	20	1.8
DC power distribution	0.5	20	0.6
pumping system for gas catcher/cooler			
clean booster pumps	48.0	10	52.8
clean backing pump	25.0	10	27.5
turbo drag pump	9.0	10	9.9
turbo pump	15.0	10	16.5
scrollpump (2)	8.0	10	8.8
vacuum gauge and control	10.0	20	12.0
dual gas purification/distribution system			
solid state purifier (2)	16.0	10	17.6
cold trap (2)	2.5	20	3.0
high purity regulators (3)	4.4	10	4.8
gas flow controller	6.0	10	6.6
VCR gas distribution system	3.5	20	4.2
on-platform ion transport and diagnostics			
high voltage acceleration section (2)	15.0	30	19.5
quads (2)	6.0	30	7.8
60 degrees bending magnet (2)	223.0	23	274.0
multipole magnet	12.0	30	15.6
regulated current power supplies	30.0	20	36.0
50 kV power supply	10.0	20	12.0
HV Transformer (50kV, 30kVA)	40.0	10	44.0
vacuum enclosure	15.0	30	19.5
pumping system and vacuum control	40.0	20	48.0
slit system	10.0	30	13.0
isobar separator diagnostics station	15.0	30	19.5
acceleration column (2)	60.0	20	72.0
removable shielding liner	5.0	30	6.5
off-platform ion transport and diagnostics station			
acceleration column	30.0	20	36.0
electrostatic bends and focusing	20.0	20	24.0
vacuum enclosure	15.0	30	19.5
pumping system and control	45.0	20	54.0
ATLAS diagnostics improvements			
Modify existing solid state detector diagnostics	15.0	20	18.0
Weak-beam profile monitors (6)	125.0	20	150.0
Weak-beam current detectors (6)	60.0	20	72.0
off-platform interface/ control console	50.0	20	60.0
shielding/radiation control/safety review	80.0	30	104.0
additional manpower required			
1 engineer for 1.5 years	309.0	10.0	339.9
1 technician for 1.5 years	255.0	10.0	280.5
1 designer for 1 year	143.0	10.0	157.3
1 post-doctoral position for 1.75 years	159.0	10.0	174.9
total cost	**2926.1**	**16.0%**	**3391.1**

IX. Schedule and Manpower

The schedule for this project is based on the assumption that funding will become available at the start of FY2006. The time required to complete construction of the project is expected to be two years. The design, procurement, fabrication, installation, assembly, and commissioning will follow the schedule as illustrated in Figure 21. To achieve this schedule, the project will need to be funded over a two year period. In the first year, FY2006, we request funding at the level of $1900k with the remainder, $1491, provide in FY2007.

Minimizing the disruption of ATLAS operation is a prime concern in the schedule. The new high-voltage platform and gas catcher/cooler assemblies will be constructed and tested independently of ATLAS operation. During the construction phase for ECR-I (about 9 months into the project), the source will be removed from normal ATLAS operation. Following restart of ECR-I, much of its running will be to commission the source as a charge breeder using simple stable-beam 1+ sources, such as surface ionization sources, for the test beams. During this period ECR-I may return to limited use for ATLAS operation as needed. The reconfiguration of ECR-I and the initial restart of the source is expected to take approximately three months.

Connection of both high-voltage platforms will be performed once both components are ready which is about 1 year into the project. Two safety reviews of the project are

proposed during the construction and installation phase with an additional final review before the 1 Ci californium source is received.

Safety reviews will be conducted regularly throughout the construction, installation and commissioning phases. Three permit-to-operate reviews are identified as milestones on the project schedule, one prior to each stage of introducing increased amounts of radioactive material.

The Physics Division manpower and additional engineering and design effort necessary for this project is estimated to be slightly over 10.5 man-years, including a project manager and technical director. This does not include machine shop and electronics shop construction effort for components contained in Table 3. Of the total effort identified in Table 4, 4.33 man-years is assumed to come from existing ATLAS staff.

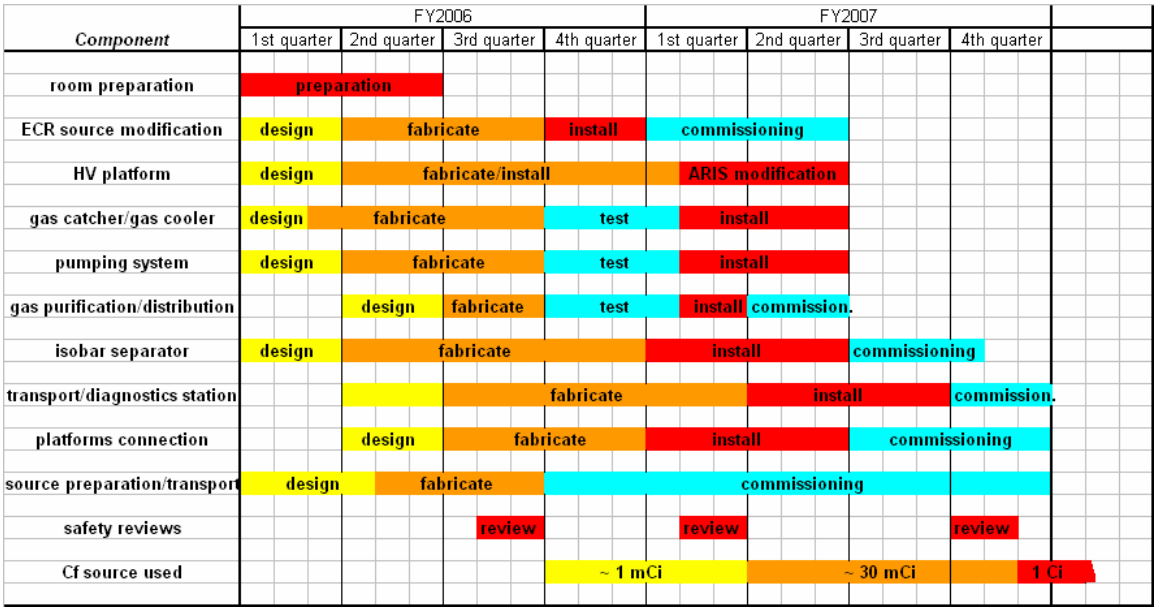

Figure 21. Schedule for the main tasks of the ATLAS californium source radioactive beam upgrade project. Radioactive beams from the upgrade should be available for experiments within just under two years.

The staffing profile assumes that the engineering and drafting effort will be obtained as temporary assignments from other ANL divisions. These positions are clearly marked in Table 4. In addition a new technician and a new post-doctoral position are indicated. These positions are new hires and it will be necessary to maintain these positions into the commissioning and operating phases of the project. The costs for these two additional positions must come from additional operating funds in outlying years. The total operating budget enhancements that will be needed to operate this new facility, including these two additional positions, capital equipment and M&S is approximately $500k.

Table 4. ^{252}Cf upgrade staffing levels during construction

	FY2006				FY2007				FY2008	Total man-month
Person	1st Qrtr	2nd Qrtr	3rd Qrtr	4th Qrtr	1st Qrtr	2nd Qrtr	3rd Qrtr	4th Qrtr		
New Designer*									Start	12
New Engineer*									comm	18
New Post Doc									ission	21
New Technician									ing	18
Redirect existing ECR Group									of	12
Project Manager									full	8
Technical Director									system	8
Computer Control (ATLAS staff)										6
Other ATLAS staff (ARIS, diagnostics, electronics, procedures, training)										18
Other ANL staff										6
Total										127

* Designer and Engineer to be 'purchased' from other ANL divisions for period required.

Full time

Part time

X. Expected Performance

The estimated yields both at low energy and after acceleration for the more abundant ^{252}Cf fission fragments are given below. The independent yields (percentage of direct fission branch) are color coded to indicate the more intense beams. Low energy beams are available at energies from about 10 keV up to 250-500 keV depending on the charge state extracted from the gas catcher system. Accelerated beams are available from these energies up to the maximum energy the ATLAS facility will be able to deliver after the current energy upgrade, roughly from ion source energy up to 12-16 MeV/u for the light fission fragments and up to 10-13 MeV/u for the heavy fragments.

The yield estimate uses the measured direct yield from a 1 Ci californium source. It assumes a 50% stopping fraction in the gas catcher, 45% extraction efficiency out of the gas catcher /gas cooler assembly, charge state breeding efficiency of 10% for gaseous species and 5% for solids, decay losses at all steps of the process (assuming 20 ms for the extraction/cooling time and 30 ms for charge breeding), 85% bunching efficiency and 90% transmission efficiency (other than bunching) through ATLAS. No significant losses are expected from the charge-state distribution after the catcher since the fission fragments will emerge predominantly in a single charge state (1+ or 2+).

Nuclide	t1/2	independent yield	low energy beam (ions/sec)	accelerated beam (ions/sec)
83As	13.4 s	2.32E-02	6.3E+04	2.3E+03
83Se	22.3m	9.01E-03	2.4E+04	8.9E+02
84As	5.5 s	2.19E-02	5.9E+04	2.2E+03
84Se	3.3 m	2.55E-02	6.9E+04	2.5E+03
85As	2.03 s	2.60E-02	7.0E+04	2.5E+03
85Se-m	19 s	3.75E-02	1.0E+05	3.7E+03
85Se	39 s	3.75E-02	1.0E+05	3.7E+03
85Br	2.87m	1.92E-02	5.2E+04	1.9E+03
86As	0.9 s	9.35E-03	2.5E+04	8.9E+02
86Se	15.0 s	6.70E-02	1.8E+05	6.6E+03
86Br-m	4.5 s	2.10E-02	5.6E+04	2.1E+03
86Br	55.5 s	2.10E-02	5.7E+04	2.1E+03
87Se	5.6 s	7.11E-02	1.9E+05	7.0E+03
87Br	55.9 s	1.10E-01	3.0E+05	1.1E+04
87Kr	1.27 h	2.24E-02	6.0E+04	4.4E+03
88Se	1.50 s	4.42E-02	1.2E+05	4.3E+03
88Br	16.4 s	1.69E-01	4.6E+05	1.7E+04
88Kr	2.84 h	8.81E-02	2.4E+05	1.7E+04
89Se	0.41 s	1.53E-02	4.0E+04	1.4E+03
89Br	4.37 s	1.50E-01	4.0E+05	1.5E+04
89Kr	3.15 m	1.74E-01	4.7E+05	3.4E+04
89Rb	15.4 m	2.00E-02	5.4E+04	2.0E+03
90Br	1.9 s	1.09E-01	2.9E+05	1.1E+04
90Kr	32.3 s	3.35E-01	9.0E+05	6.6E+04
90Rb-m	4.3 m	7.48E-02	2.0E+05	7.4E+03
90Rb	2.6 m	1.75E-02	4.7E+04	1.7E+03
91Br	0.54 s	4.14E-02	1.1E+05	3.8E+03
91Kr	8.6 s	3.16E-01	8.5E+05	6.2E+04
91Rb	58.0 s	2.24E-01	6.0E+05	2.2E+04
91Sr	9.5 h	1.78E-02	4.8E+04	1.8E+03
92Br	0.34 s	1.20E-02	3.1E+04	1.1E+03
92Kr	1.84 s	2.36E-01	6.3E+05	4.6E+04
92Rb	4.48 s	3.47E-01	9.3E+05	3.4E+04
92Sr	2.71 h	8.14E-02	2.2E+05	8.1E+03
93Kr	1.29 s	1.30E-01	3.5E+05	2.5E+04
93Rb	5.85 s	5.03E-01	1.4E+06	4.9E+04
93Sr	7.4 m	2.36E-01	6.4E+05	2.3E+04
93Y	10.2 h	1.07E-02	2.9E+04	1.1E+03
94Kr	0.21 s	4.89E-02	1.2E+05	8.1E+03
94Rb	2.73 s	4.54E-01	1.2E+06	4.4E+04
94Sr	1.25 m	5.47E-01	1.5E+06	5.4E+04
94Y	18.7 m	5.96E-02	1.6E+05	5.9E+03
95Kr	0.78 s	1.10E-02	2.9E+04	2.1E+03
95Rb	0.377s	2.68E-01	6.9E+05	2.4E+04

95Sr	25.1s	7.67E-01	2.1E+06	7.6E+04
95Y	10.3 m	1.98E-01	5.3E+05	2.0E+04
96Rb	0.199s	1.27E-01	3.1E+05	1.0E+04
96Sr	1.06 s	8.88E-01	2.4E+06	8.5E+04
96Y -m	9.6 s	4.91E-01	1.3E+06	4.8E+04
96Y	6.2 s	5.45E-02	1.5E+05	5.4E+03
97Rb	0.169s	3.44E-02	8.4E+04	2.7E+03
97Sr	0.42 s	6.02E-01	1.6E+06	5.4E+04
97Y	3.76 s	8.70E-01	2.3E+06	8.5E+04
97Zr	16.8 h	1.66E-01	4.5E+05	1.6E+04
98Rb	0.107s	8.20E-03	1.9E+04	5.7E+02
98Sr	0.65 s	3.71E-01	9.8E+05	3.5E+04
98Y -m	2.1 s	6.43E-01	1.7E+06	6.3E+04
98Y	0.59 s	6.43E-01	1.7E+06	6.0E+04
98Zr	30.7 s	5.87E-01	1.6E+06	5.8E+04
98Nb	2.9 s	1.62E-02	4.3E+04	1.6E+03
99Sr	0.269s	1.35E-01	3.4E+05	1.2E+04
99Y	1.47 s	1.15E+00	3.1E+06	1.1E+05
99Zr	2.2 s	1.25E+00	3.3E+06	1.2E+05
99Nb-m	2.6 m	1.07E-01	2.9E+05	1.1E+04
99Nb	15.0 s	9.33E-03	2.5E+04	9.2E+02
100Sr	0.201s	3.52E-02	8.7E+04	2.9E+03
100Y	0.73 s	7.78E-01	2.1E+06	7.3E+04
100Zr	7.1 s	2.06E+00	5.5E+06	2.0E+05
100Nb-m	3.0 s	2.85E-01	7.7E+05	2.8E+04
100Nb	1.5 s	2.85E-01	7.6E+05	2.8E+04
100Mo	stable	1.48E-02	4.0E+04	1.5E+03
101Y	0.43 s	3.36E-01	8.7E+05	3.0E+04
101Zr	2.1 s	2.20E+00	5.9E+06	2.1E+05
101Nb	7.1 s	1.30E+00	3.5E+06	1.3E+05
101Mo	14.6 m	8.93E-02	2.4E+05	8.8E+03
102Y	0.36 s	8.26E-02	2.1E+05	7.4E+03
102Zr	2.9 s	1.45E+00	3.9E+06	1.4E+05
102Nb	1.3 s	2.04E+00	5.4E+06	2.0E+05
102Mo	11.3 m	4.64E-01	1.3E+06	4.6E+04
103Y	0.260s	1.78E-02	4.5E+04	1.5E+03
103Zr	1.3 s	8.43E-01	2.2E+06	8.1E+04
103Nb	1.5 s	3.06E+00	8.2E+06	3.0E+05
103Mo	1.13 m	1.47E+00	4.0E+06	1.5E+05
103Tc	54 s	5.66E-02	1.5E+05	5.6E+03
104Zr	1.2 s	2.24E-01	6.0E+05	2.1E+04
104Nb	4.8 s	2.15E+00	5.8E+06	2.1E+05
104Mo	60 s	2.83E+00	7.6E+06	2.8E+05
104Tc	18.2 m	4.31E-01	1.2E+06	4.3E+04
105Zr	0.493s	3.91E-02	1.0E+05	3.6E+03
105Nb	3.0 s	9.99E-01	2.7E+06	9.8E+04
105Mo	36 s	3.02E+00	8.2E+06	3.0E+05
105Tc	7.6 m	2.10E+00	5.7E+06	2.1E+05
105Ru	4.44 h	6.83E-02	1.8E+05	6.8E+03
106Nb	1.0 s	4.41E-01	1.2E+06	4.2E+04

106Mo	8.4 s	3.47E+00	9.3E+06	3.4E+05
106Tc	36 s	2.19E+00	5.9E+06	2.2E+05
106Ru	1.020y	2.08E-01	5.6E+05	2.1E+04
107Nb	0.766s	9.02E-02	2.4E+05	8.5E+03
107Mo	3.5 s	2.01E+00	5.4E+06	2.0E+05
107Tc	21.2 s	3.63E+00	9.8E+06	3.6E+05
107Ru	3.8 m	8.72E-01	2.4E+06	8.6E+04
107Rh	21.7 m	1.58E-02	4.3E+04	1.6E+03
108Nb	0.242s	1.02E-02	2.6E+04	8.6E+02
108Mo	1.5 s	6.67E-01	1.8E+06	6.4E+04
108Tc	5.1 s	3.33E+00	9.0E+06	3.3E+05
108Ru	4.5 m	1.98E+00	5.3E+06	2.0E+05
108Rh-m	5.9 m	5.73E-02	1.5E+05	5.7E+03
108Rh	17 s	5.73E-02	1.5E+05	5.7E+03
109Mo	1.41 s	1.48E-01	3.9E+05	1.4E+04
109Tc	1.4 s	1.89E+00	5.0E+06	1.8E+05
109Ru	34.5 s	2.99E+00	8.1E+06	3.0E+05
109Rh-m	50 s	2.54E-01	6.9E+05	2.5E+04
109Rh	1.34 m	6.52E-01	1.8E+06	6.5E+04
110Mo	2.77 s	2.31E-02	6.2E+04	2.3E+03
110Tc	0.83 s	8.55E-01	2.3E+06	8.1E+04
110Ru	15 s	3.62E+00	9.8E+06	3.6E+05
110Rh-m	29 s	6.75E-01	1.8E+06	6.7E+04
110Rh	3.1 s	6.72E-01	1.8E+06	6.6E+04
110Pd	stable	6.05E-02	1.6E+05	6.0E+03
111Tc	1.98 s	1.76E-01	4.7E+05	1.7E+04
111Ru	1.5 s	2.26E+00	6.0E+06	2.2E+05
111Rh	11 s	2.46E+00	6.6E+06	2.4E+05
111Pd-m	5.5 h	1.71E-01	4.6E+05	1.7E+04
111Pd	23.4 m	1.21E-01	3.3E+05	1.2E+04
112Tc	0.431s	2.29E-02	5.9E+04	2.1E+03
112Ru	4.5 s	9.39E-01	2.5E+06	9.2E+04
112Rh	4 s	2.39E+00	6.4E+06	2.3E+05
112Pd	20.04h	7.45E-01	2.0E+06	7.4E+04
112Ag	3.13 h	3.60E-02	9.7E+04	3.6E+03
113Ru	2.7 s	2.13E-01	5.7E+05	2.1E+04
113Rh	0.9 s	1.95E+00	5.2E+06	1.9E+05
113Pd	1.64 m	2.39E+00	6.5E+06	2.4E+05
113Ag-m	1.14 m	1.96E-01	5.3E+05	1.9E+04
113Ag	5.3 h	2.94E-02	7.9E+04	2.9E+03
114Ru	8.14 s	1.90E-02	5.1E+04	1.9E+03
114Rh	1.8 s	5.60E-01	1.5E+06	5.4E+04
114Pd	2.48 m	1.82E+00	4.9E+06	1.8E+05
114Ag	4.6 s	9.13E-01	2.5E+06	9.0E+04
114Cd	stable	1.98E-02	5.3E+04	2.0E+03
115Rh	0.99 s	1.71E-01	4.5E+05	1.6E+04
115Pd	47 s	1.70E+00	4.6E+06	1.7E+05
115Ag-m	18.7 s	5.38E-01	1.5E+06	5.3E+04
115Ag	20 m	4.39E-01	1.2E+06	4.3E+04
115Cd-m	44.6 d	4.10E-02	1.1E+05	4.1E+03

115Cd	2.228d	1.23E-02	3.3E+04	1.2E+03
116Rh	0.7 s	2.26E-02	6.0E+04	2.1E+03
116Pd	12.7 s	8.19E-01	2.2E+06	8.1E+04
116Ag-m	10.5 s	5.37E-01	1.4E+06	5.3E+04
116Ag	2.68 m	6.50E-01	1.8E+06	6.4E+04
116Cd	stable	9.83E-02	2.7E+05	9.7E+03
117Pd	5 s	2.92E-01	7.9E+05	2.9E+04
117Ag-m	5.3 s	5.15E-01	1.4E+06	5.1E+04
117Ag	1.22 m	5.00E-01	1.3E+06	4.9E+04
117Cd-m	3.4 h	1.47E-01	4.0E+05	1.5E+04
117Cd	2.49 h	4.38E-02	1.2E+05	4.3E+03
118Pd	2.4 s	1.27E-01	3.4E+05	1.2E+04
118Ag-m	2.4 s	2.94E-01	7.9E+05	2.9E+04
118Ag	4.0 s	2.97E-01	8.0E+05	2.9E+04
118Cd	50.3 m	2.72E-01	7.3E+05	2.7E+04
119Pd	1.76 s	8.49E-03	2.3E+04	8.2E+02
119Ag	2.1s	1.93E-01	5.2E+05	1.9E+04
119Cd-m	2.20 m	8.91E-02	2.4E+05	8.8E+03
119Cd	2.69 m	8.91E-02	2.4E+05	8.8E+03
120Ag	1.23 s	7.95E-02	2.1E+05	7.6E+03
120Cd	50.8 s	1.56E-01	4.2E+05	1.5E+04
121Ag	0.78 s	1.90E-02	5.0E+04	1.8E+03
121Cd	13.5 s	9.79E-02	2.6E+05	9.7E+03
122Cd	5.3 s	8.34E-02	2.2E+05	8.2E+03
123Cd	2.09 s	3.34E-02	8.9E+04	3.2E+03
124Cd	1.24 s	1.10E-02	2.9E+04	1.1E+03
124In	3.18 s	9.46E-03	2.5E+04	9.3E+02
126In	1.63 s	7.98E-03	2.1E+04	7.7E+02
126Sn	1.e5y	1.77E-02	4.8E+04	1.8E+03
127Sn-m	4.15 m	2.85E-02	7.7E+04	2.8E+03
127Sn	2.12 h	6.97E-02	1.9E+05	6.9E+03
128Sn	59.1 m	1.75E-01	4.7E+05	1.7E+04
128Sb-m	10.1 m	9.48E-03	2.6E+04	9.4E+02
129Sn-m	6.9 m	1.18E-01	3.2E+05	1.2E+04
129Sn	2.4 m	2.88E-01	7.8E+05	2.9E+04
129Sb	4.40 h	1.72E-01	4.6E+05	1.7E+04
130In	0.29 s	1.02E-02	2.6E+04	8.9E+02
130Sn	3.7 m	3.62E-01	9.8E+05	3.6E+04
130Sb-m	6.5 m	2.80E-01	7.6E+05	2.8E+04
130Sb	38.4 m	1.64E-01	4.4E+05	1.6E+04
130Te	stable	3.07E-02	8.3E+04	3.0E+03
131Sn	39 s	2.96E-01	8.0E+05	2.9E+04
131Sb	23.0 m	9.95E-01	2.7E+06	9.9E+04
131Te-m	1.35 d	2.36E-01	6.4E+05	2.3E+04
131Te	25.0 m	6.95E-02	1.9E+05	6.9E+03
132Sn	40 s	1.38E-01	3.7E+05	1.4E+04
132Sb-m	2.8 m	5.11E-01	1.4E+06	5.1E+04
132Sb	4.2 m	7.06E-01	1.9E+06	7.0E+04
132Te	3.26 d	7.77E-01	2.1E+06	7.7E+04
132I	2.28 h	2.11E-02	5.7E+04	2.1E+03

133Sn	1.44 s	6.26E-02	1.7E+05	6.0E+03
133Sb	2.5 m	1.06E+00	2.9E+06	1.0E+05
133Te-m	55.4 m	1.28E+00	3.5E+06	1.3E+05
133Te	12.4 m	5.24E-01	1.4E+06	5.2E+04
133I	20.8 h	2.19E-01	5.9E+05	2.2E+04
134Sn	1.04 s	1.51E-02	4.0E+04	1.4E+03
134Sb	0.8 s	5.58E-01	1.5E+06	5.3E+04
134Te	42 m	2.35E+00	6.3E+06	2.3E+05
134I -m	3.7 m	5.83E-01	1.6E+06	5.8E+04
134I	52.6 m	3.31E-01	8.9E+05	3.3E+04
134Xe-m	0.29 s	2.60E-02	6.6E+04	4.5E+03
135Sb	1.71 s	1.46E-01	3.9E+05	1.4E+04
135Te	19.0 s	1.78E+00	4.8E+06	1.8E+05
135I	6.57 h	1.85E+00	5.0E+06	1.8E+05
135Xe-m	15.3 m	2.25E-01	6.1E+05	4.4E+04
135Xe	9.10 h	1.86E-01	5.0E+05	3.7E+04
136Sb	0.82 s	3.02E-02	8.0E+04	2.9E+03
136Te	17.5 s	9.12E-01	2.5E+06	9.0E+04
136I -m	47 s	9.32E-01	2.5E+06	9.2E+04
136I	1.39 m	1.36E+00	3.7E+06	1.3E+05
137Te	2.5 s	2.33E-01	6.2E+05	2.3E+04
137I	24.5 s	1.57E+00	4.2E+06	1.6E+05
137Xe	3.82 m	2.59E+00	7.0E+06	5.1E+05
137Cs	30.17y	6.93E-01	1.9E+06	6.9E+04
138Te	1.4 s	5.41E-02	1.4E+05	5.2E+03
138I	6.5 s	1.00E+00	2.7E+06	9.8E+04
138Xe	14.1 m	3.63E+00	9.8E+06	7.2E+05
138Cs-m	2.9 m	3.01E-01	8.1E+05	3.0E+04
138Cs	32.2 m	5.73E-01	1.5E+06	5.7E+04
139Te	0.580s	8.22E-03	2.2E+04	7.6E+02
139I	2.30 s	4.10E-01	1.1E+06	4.0E+04
139Xe	39.7 s	3.50E+00	9.4E+06	6.9E+05
139Cs	9.3 m	1.83E+00	4.9E+06	1.8E+05
139Ba	1.396h	1.45E-01	3.9E+05	1.4E+04
140I	0.86 s	1.16E-01	3.1E+05	1.1E+04
140Xe	13.6 s	2.55E+00	6.9E+06	5.0E+05
140Cs	1.06 m	2.77E+00	7.5E+06	2.7E+05
140Ba	12.75d	5.16E-01	1.4E+06	5.1E+04
141I	0.45s	2.77E-02	7.2E+04	2.5E+03
141Xe	1.72 s	1.00E+00	2.7E+06	1.9E+05
141Cs	24.9 s	3.79E+00	1.0E+07	3.7E+05
141Ba	18.3 m	1.11E+00	3.0E+06	1.1E+05
141La	3.90 h	3.72E-02	1.0E+05	3.7E+03
142Xe	1.22 s	3.68E-01	9.8E+05	7.0E+04
142Cs	1.8 s	2.53E+00	6.8E+06	2.5E+05
142Ba	10.7 m	2.70E+00	7.3E+06	2.7E+05
142La	1.54 h	4.14E-01	1.1E+06	4.1E+04
143Xe	0.30 s	4.18E-02	1.1E+05	7.3E+03
143Cs	1.78 s	7.43E-01	2.0E+06	7.2E+04
143Ba	14.3 s	4.40E+00	1.2E+07	4.3E+05

143La	14.1 m	1.05E+00	2.8E+06	1.0E+05
143Ce	1.38 d	1.64E-02	4.4E+04	1.6E+03
144Xe	1.2 s	1.16E-02	3.1E+04	2.2E+03
144Cs	1.01 s	5.49E-01	1.5E+06	5.2E+04
144Ba	11.4 s	3.37E+00	9.1E+06	3.3E+05
144La	40.7 s	1.86E+00	5.0E+06	1.8E+05
144Ce	284.6d	1.01E-01	2.7E+05	1.0E+04
145Cs	0.59 s	1.49E-01	3.9E+05	1.4E+04
145Ba	4.0 s	2.06E+00	5.5E+06	2.0E+05
145La	24 s	2.51E+00	6.8E+06	2.5E+05
145Ce	3.00 m	3.47E-01	9.4E+05	3.4E+04
146Cs	0.322s	2.58E-02	6.6E+04	2.3E+03
146Ba	2.20 s	9.81E-01	2.6E+06	9.5E+04
146La	6.3 s	2.39E+00	6.4E+06	2.4E+05
146Ce	13.5 m	1.01E+00	2.7E+06	1.0E+05
146Pr	24.2 m	3.07E-02	8.3E+04	3.0E+03
147Ba	0.892s	2.50E-01	6.6E+05	2.4E+04
147La	4.02 s	1.94E+00	5.2E+06	1.9E+05
147Ce	56 s	1.91E+00	5.2E+06	1.9E+05
147Pr	13.4 m	1.81E-01	4.9E+05	1.8E+04
148Ba	0.64 s	4.80E-02	1.3E+05	4.5E+03
148La	1.1 s	9.86E-01	2.6E+06	9.4E+04
148Ce	56 s	2.35E+00	6.3E+06	2.3E+05
148Pr	2.27 m	5.41E-01	1.5E+06	5.4E+04
148Nd	stable	1.33E-02	3.6E+04	1.3E+03
149La	1.10 s	2.34E-01	6.2E+05	2.2E+04
149Ce	5.2 s	1.50E+00	4.0E+06	1.5E+05
149Pr	2.3 m	9.29E-01	2.5E+06	9.2E+04
149Nd	1.72 h	5.80E-02	1.6E+05	5.7E+03
150La	0.608s	5.51E-02	1.4E+05	5.1E+03
150Ce	4.4 s	9.41E-01	2.5E+06	9.2E+04
150Pr	6.2 s	1.30E+00	3.5E+06	1.3E+05
150Nd	stable	1.45E-01	3.9E+05	1.4E+04
151Ce	1.0 s	2.92E-01	7.7E+05	2.8E+04
151Pr	22.4 s	1.07E+00	2.9E+06	1.1E+05
151Nd	12.4 m	5.60E-01	1.5E+06	5.5E+04
151Pm	1.183d	2.15E-02	5.8E+04	2.1E+03
152Ce	3.1 s	7.45E-02	2.0E+05	7.3E+03
152Pr	3.2 s	6.96E-01	1.9E+06	6.8E+04
152Nd	11.4 m	8.28E-01	2.2E+06	8.2E+04
152Pm-m	7.5 m	6.06E-02	1.6E+05	6.0E+03
152Pm	4.1 m	6.06E-02	1.6E+05	6.0E+03
153Ce	1.47 s	1.02E-02	2.7E+04	9.8E+02
153Pr	4.3 s	2.61E-01	7.0E+05	2.6E+04
153Nd	28.9 s	7.99E-01	2.2E+06	7.9E+04
153Pm	5.4 m	2.17E-01	5.9E+05	2.1E+04
154Pr	2.3 s	5.33E-02	1.4E+05	5.2E+03
154Nd	25.9 s	4.19E-01	1.1E+06	4.1E+04
154Pm-m	2.7 m	2.55E-01	6.9E+05	2.5E+04
154Pm	1.7 m	2.98E-01	8.0E+05	2.9E+04

154Sm	stable	4.19E-02	1.1E+05	4.1E+03
155Pr	1.12 s	1.15E-02	3.1E+04	1.1E+03
155Nd	8.9 s	2.43E-01	6.5E+05	2.4E+04
155Pm	48 s	4.40E-01	1.2E+06	4.4E+04
155Sm	22.2 m	9.59E-02	2.6E+05	9.5E+03
156Nd	5.5 s	1.05E-01	2.8E+05	1.0E+04
156Pm	26.7 s	4.58E-01	1.2E+06	4.5E+04
156Sm	9.4 h	1.01E-01	2.7E+05	1.0E+04
156Eu	15.2 d	9.92E-03	2.7E+04	9.8E+02
157Nd	2.48 s	1.77E-02	4.7E+04	1.7E+03
157Pm	10.9 s	2.00E-01	5.4E+05	2.0E+04
157Sm	8.0 m	2.85E-01	7.7E+05	2.8E+04
157Eu	15.13h	3.50E-02	9.4E+04	3.5E+03
158Pm	4.8 s	6.91E-02	1.9E+05	6.8E+03
158Sm	5.5 m	2.45E-01	6.6E+05	2.4E+04
158Eu	45.9 m	1.48E-01	4.0E+05	1.5E+04
159Pm	3.0 s	2.04E-02	5.5E+04	2.0E+03
159Sm	11.3 s	1.76E-01	4.7E+05	1.7E+04
159Eu	18.1 m	1.31E-01	3.5E+05	1.3E+04
159Gd	18.6 h	1.24E-02	3.3E+04	1.2E+03
160Sm	9.6 s	8.67E-02	2.3E+05	8.5E+03
160Eu	38 s	1.57E-01	4.2E+05	1.6E+04
160Gd	stable	3.74E-02	1.0E+05	3.7E+03
161Sm	4.78 s	2.49E-02	6.7E+04	2.4E+03
161Eu	27 s	1.06E-01	2.9E+05	1.0E+04
161Gd	3.66 m	5.95E-02	1.6E+05	5.9E+03
162Eu	11 s	4.70E-02	1.3E+05	4.6E+03
162Gd	8.4 m	6.10E-02	1.6E+05	6.0E+03
163Eu	7.60 s	1.52E-02	4.1E+04	1.5E+03
163Gd	1.13 m	4.68E-02	1.3E+05	4.6E+03
163Tb	19.5 m	1.28E-02	3.5E+04	1.3E+03
164Gd	45 s	2.58E-02	7.0E+04	2.6E+03
164Tb	3.0 m	1.65E-02	4.5E+04	1.6E+03
165Gd	0.705m	9.96E-03	2.7E+04	9.9E+02
165Tb	2.1 m	1.51E-02	4.1E+04	1.5E+03
166Tb	~ 1 m	1.04E-02	2.8E+04	1.0E+03

XI. References

1. A.H. Wuosmaa *et al.*, *Proposal for a solenoidal spectrometer to study reactions with short-lived beams*. submitted to DOE in October 2004.
2. D.C. Radford *et al., Physics with heavy neutron-rich RIBs at the HRIBF*, Eur. Phys. J. **A15**, 171 (2002).
3. H.-J. Kluge, W. Nörtershäuser, *Lasers for nuclear physics*, Spectrochimica Acta Part B **58,** 1031 (2003).
4. F. Le Blanc *et al.*, *Charge radii and nuclear moments around Sn-132*, Nucl. Phys. A **734**, 437 (2004).
5. J.M.G. Levins *et al.*, *First On-Line Laser Spectroscopy of Radioisotopes of a Refractory Element*, Phys. Rev. Lett. **82**, 2476 (1999).
6. R. Geller, C. Tamburella, and J.L. Belmont, *The ISOL-MAFIOS Source,* Rev. Sci Instrum., **67(3),** 1281(1996).
7. T. Lamy *et al., Charge state breeding applications with the ECR PHOENIX source: From low to high current production,* Rev. Sci. Instrum, **73(2)**, 717(2002).
8. T. Lamy, *et al., Charge Breeeding Method Results with the Phoenix Booster ECR Ion Source,* Proceedings EPAC 2002, Paris France, June 3-7, 2002, pp. 1724-1726.
9. G. Savard *et al., Development and Operation of Gas Catchers to Thermalize Fusion-evaporation and Fragmentation Products*, Nucl. Instr. & Meth. **B204,** 582 (2003).
10. F. Herfurth *et al., A linear radiofrequency ion trap for accumulation, bunching, and emittance improvement of radioactive ion beams,* Nucl. Instr. & Meth. **A469**, 254 (2001).
11. M. Portillo, J.A. Nolen and T.A. Barlow, *Design layout of an isobar separator based on 5th order calculations*, in Proceedings of the 2001 IEEE Particle Accelerator Conference, edited by P. Lucas and S. Webber, Chicago, IL, June 18-22 2001, pp. 3015-3017.
12. R.A. Anderl *et al.*, *Ion-source development at the ^{252}Cf ISOL facility*, Nucl. Instr. and Meth. B26 (1987) 333.
13. R.A. Anderl *et al., A laboratory-scale shielded cell for ^{252}Cf*, Proc. 27th Conf. Remote Systems Technology (1979) p. 347.
14. F. Wenander, *Charge Breeding Techniques,* Nuclear Physics **A746,** 40c (2004).